COMPOSITE ELECTRODES WITH IMMOBILIZED BACTERIA BIOANODE AND PHOTOSYNTHETIC ALGAE BIOCATHODE FOR BIO-BATTERIES

A Thesis Submitted to the College of

Graduate Studies and Research

In Partial Fulfillment of the Requirements

For the Degree of Master of Science in the

Department of Chemical and Biological Engineering

University of Saskatchewan

Saskatoon

By

Siddharth Suresh

Permission to Use

In presenting this thesis in partial fulfillment of the requirements for a Postgraduate degree from the University of Saskatchewan, I agree that the Libraries of this University may make it freely available for inspection. I further agree that permission for copying of this thesis in any manner, in whole or in part, for scholarly purposes may be granted by Dr. Richard Evitts who supervised my thesis work or, in his absence, by the Head of the Department or the Dean of the College of Engineering. It is understood that any copying or publication or use of this thesis or parts thereof for financial gain shall not be allowed without my written permission. It is also understood that due recognition shall be given to me and to the University of Saskatchewan in any scholarly use which may be made of any material in my thesis.

Requests for permission to copy or to make other use of material in this thesis in whole or part should be addressed to:

Head of the Department of Chemical and Biological Engineering

University of Saskatchewan

Saskatoon, Saskatchewan S7N 5A9

Canada

ABSTRACT

A novel electrode was constructed and tested in a bio-battery. This configuration consisted of a composite electrode with immobilized bacteria (*Escherichia coli K-12*) in the anode and a composite electrode with immobilized Carbon Nanoparticles (CNP) and algae *(Chlorella vulgaris/Scenedesmus sp.)* suspended in the cathode. The composite electrode consisted of three parts: a 304L stainless steel mesh base, an electro-polymerized layer of pyrrole, and an electro-polymerized layer of methylene blue. The bacteria were immobilized on the anode electrode using a technique incorporating CNP and a Teflon^{tm} emulsion. The anode and cathode electrodes were tested separately in conjunction with chemical cathodes and anodes respectively.

The composite electrode with immobilized bacteria was tested in a bioanode setup. The cathode chamber of the cell contained a potassium ferricyanide and buffer solution with a graphite electrode. Factors affecting electrode performance, such as Teflon^{tm} and carbon nanoparticle concentration, were investigated to find optimum values. The maximum power density generated by the composite electrode with immobilized bacteria and a chemical cathode was 378 mW/m^2. This electrode configuration produced approximately 69% more power density and 53% more current density than composite electrodes with bacteria suspended in solution. Electrochemical Impedance Spectroscopy analysis determined that a significant portion of the bio-battery's resistance to charge transfer occurred at the surface of the anode and this resistance was significantly lowered when using immobilized bacteria (51% lower than bio-batteries with suspended bacteria).

Similarly, biocathodes containing composite electrodes coated with CNP were tested using two algae species, *Chlorella vulgaris* and *Scenedesmus sp.*, suspended in solution. This electrode configuration was compared with composite electrode without CNP coating. The anode chamber

contained potassium ferrocyanide solution with a graphite counter electrode. The composite electrode with CNP produced approximately 23% more current density than composite electrode without CNP.

A complete bio-battery was designed using a composite electrode with immobilized bacteria anode and a CNP coated composite electrode with algae suspended in the cathode. EIS analysis showed that the resistance was higher in the biocathode than in the bioanode and a significant portion of the ohmic resistance was contributed by the membrane.

ACKNOWLEDGMENTS

I would like to express my sincere appreciation to my supervisor, Dr. Richard Evitts for his continuous support, interest, patience and encouragement for my Masters work. I would also like to thank my advisory committee, Dr. Mehdi Nemati and Dr. Aaron Phoenix for their thoughts and valuable advices. Also, to Natural Sciences and Engineering Research Council of Canada for their financial support.

I would also like to thank Dragan Cekic, Rlee Prokopishyn and the Engineering workshop staff for helping me purchase and setup my experimental equipment. Also, to fellow graduate students Naveenji Arun, Lyman Moreno and Manjunathan Ulaganathan for their help and friendship.

Finally, this work is dedicated to my dear parents for their love and encouragement during the past years.

TABLE OF CONTENTS

LIST OF TABLES

LIST OF FIGURES

NOMENCLATURE

Symbols

F	Faraday constant	C/mol
ΔG	Gibbs free energy change	-
I	Current	A
n	Number of electrons	-
R	Ideal gas constant	J/mol K
R_Ω	Ohmic resistance	Ω
R_{ct}	Charge transfer resistance	Ω
W	Warburg (Zhang *et al.*) Impedance	Ω
Y_{oc}	Constant phase element of the cathode	S
Y_o	Constant phase element of the anode	S
Z	Impedance	Ω
Z_{Re}	Real component of impedance	Ω
Z_m	Imaginary component of impedance	Ω
φ	Phase angle	°
ω	Frequency	Hz, s^{-1}
Π	Reaction quotient	varies

*S- Siemens

LIST OF ABBREVIATIONS

AC	Alternating Current (used in EIS)
CNP	Carbon Nanoparticles
CPE	Constant phase element (used in EIS modeling)
CV	Cyclic Voltammetry
DC	Direct Current (used in EIS)
EIS	Electrochemical Impedance Spectroscopy
MFC	Microbial Fuel Cell
NADH	Nicotinamide Adenine Dinucleotide (reduced)
OCP/OCV	Open Circuit Potential/Voltage
PANI	Poly(aniline)
pPy	Poly(pyrrole)
SCE	Saturated Calomel (reference) Electrode
SSM	Stainless Steel Mesh

1. INTRODUCTION

1.1 Background

Alternative methods of energy production are being investigated as potential solutions to energy-related problems. Microbial Fuel Cells (MFCs) are an emerging technology that have gained interest over the past decade as a potential source of energy (Rabaey and Verstraete, 2005). Microbial fuel cells and bio-batteries use microorganisms that catalytically oxidize the complex carbon substrates to convert chemical energy into electrical energy. The primary distinction between MFCs and bio-batteries is the substrate that gets replenished either intermittently or continuously in the MFC, while this is not the case for bio-batteries (Hoffman *et al.,* 2013).

Mediators are frequently used in MFC to enable and/or enhance electron transfer and these chemicals are often introduced into the aqueous phase in the fuel cell. One of the primary benefits of using a mediator in a MFC is its ability to lower the anode potential compared to mediator-less MFC, which lose appreciable energy during intracellular electron transfer (Yuan *et al.,* 2009). Recently polyviologen (mediator) was immobilized on a carbon cloth anode and produced a power density as high as 540 mW/m^2, normalized to a 2-D projected surface area of 7.0 cm^2 and a current density of 1.7 A/m^2 (Kim *et al.,* 2011). Prieto-Simón and Fàbregas (2004) analyzed the influence of mediators by researching the variations between mediators in epoxy composites, mediators suspended in solution, and mediators adsorbed or polymerized on electrode surfaces in biosensors. They found that mediators polymerized on electrode surfaces performed better due to their sustainable and reproducible results.

Graphite rod electrodes, which are used frequently in laboratory electrochemical studies, are generally brittle and cannot be employed for large scale processes. Hoffman *et al.* (2013) compared composite electrodes (formed from a stainless steel rod coated with polypyrrole and methylene blue) with bare graphite rod electrodes in an *E. coli K-12* based bio-battery and determined that the composite electrodes produced a 6-fold increase in power density over bare graphite rod electrodes.

Bio-films generally require significant time to establish and can cause difficulties in reproducibility (Lies *et al.*, 2005). Immobilization of bacteria directly on electrode surfaces, when compared with traditional bio-film formation may improve the electron transfer rate and reduce the start-up time of the fuel cells. Bacteria immobilization on the electrodes directly instead of bio-film formation has been studied by other researchers. Yuan *et al.* (2011) immobilized *Proteus vulgaris* on carbon paper electrodes in a mediator-less setup and achieved a maximum power density of 269 mW/m^2 by reducing the startup time of the fuel cell. A newer technique of bacteria immobilization using glycerol amended latex on carbon cloth surfaces was successfully tested and did not affect the exoelectrogenic activity (electron transfer from the cells) (Wagner *et al.*, 2012). Another interesting technique adopted by Luckarift *et al.* (2010), using vapor deposition of silica to immobilize *Shewanella oneidensis*, helped to characterize bacterial physiology and bio-electrochemical activity.

Photosynthetic biocathodes can be used for the direct production of oxygen. Powell *et al.* (2011) successfully used photosynthetic *Chlorella vulgaris* biocathodes with methylene blue as mediator in a dual chambered biological fuel cell. Moreover, an oxygenic bio-film formed on carbon veil electrodes produced a stable current upon illumination, thereby proving the power generating capabilities of photosynthetic microorganisms (Walter *et al.*, 2013).

1.2 Motivation

Although dual chambered microbial cells have been studied by various researchers in the past, multiple aspects must still be investigated, such as developing novel electrodes, to make them cost effective and efficient for the purpose of electricity generation. One major problem that has arisen when scaling up microbial fuel cells is the durability of the electrode material as commonly-used graphite rod electrodes are relatively fragile. For electrode construction, noble metals such as platinum and gold provide good results, but they are expensive. This work takes inspiration from Godwin *et al.,* 2011 who used composite electrodes (stainless steel rods polymerized with pyrrole and methylene blue) in a photosynthetic algae biocathode and these electrodes performed better than graphite rod and glassy carbon electrodes polymerized with a mediator (methylene blue). Also, these composite electrodes performed better than plain graphite electrodes in bioanodes containing *E. coli K-12* and *Shewanella oneidensis* (Hoffman *et al*., 2013).

Bio-films formed on the electrodes improve the power output of biological fuel cells. However, these bio-films take a significant time to form and often cause difficulties in result reproducibility (Lies *et al.,* 2005). Bacteria immobilization directly on the electrode instead of bio-film formation reduces the start-up time of the fuel cells (Yuan et al., 2009). In this research work the concept of bacteria immobilization on the electrode was inspired from the work done by Yuan *et al.,* 2009, who used carbon nanoparticles and Teflon^{tm} to bind the bacterial cells (*Proteus vulgaris*) on the surface of carbon paper electrodes. In the current study, the mediator (methylene blue) and bacteria (*E. coli K-12*) were immobilized on type 304 stainless steel mesh base for use as anodes.

1.3 Thesis objectives

The main objective of this research work was to create a novel electrode for improving the electricity generation of bio-batteries. This research was divided into two phases. The main goal of the first phase was to design a novel composite anode with immobilized bacteria and test it with a chemical cathode. The performance of the composite electrodes with immobilized bacteria were compared with control setups containing composite electrodes with and without CNP coating and bacteria suspended in the solution to determine the performance enhancement caused by the immobilization of mediator and bacteria.

The second phase of the research was to test the photosynthetic biocathodes containing two different composite electrode configurations (composite electrodes with and without CNP) and two different species of photosynthetic algae (*Chlorella vulgaris and Scenedesmus sp*.). The final goal was to couple the bacterial bioanodes and photosynthetic biocathodes to form a complete bio-battery and test the performance of the modified composite electrodes.

1.4 Thesis organization

The following is an outline of the remaining chapters of this thesis. Chapter Two is the literature review, background and theory. Topics related to Microbial fuel Cells (MFCs) and bio-batteries, electrode types, redox dyes (mediators), carbon nanoparticles and electrode conductivity enhancement, biocathodes and photosynthetic cathodes, impedance measurement and general analysis of the fuel cells are discussed.

Chapter Three is a detailed description of the equipment and experimental methods used in this project. First a brief description of the preparation and testing of the composite electrodes is

given and this is followed by a description of the bacteria immobilization technique, substrate concentration analysis, bioanode, biocathode and bio-battery setup and analyses.

Chapter Four is a discussion of this research work. Performance of the bioanodes and biocathodes using different electrode configurations and bio-batteries are studied by electrochemical analyses.

Chapter Five contains the summary and conclusions derived from this project. Recommendations for future work to improve the performance are also included.

2. LITERATURE REVIEW

This chapter includes the literature review, the background and theory of topics covering bio-batteries, electrode types, redox dyes (mediators), carbon nanoparticles and electrode conductivity enhancement, biocathodes and photosynthetic cathodes, impedance measurement and general analysis of fuel cells.

2.1 Microbial Fuel Cells and bio-batteries

Microbial Fuel Cells (MFCs) and bio-batteries have gained interest among researchers over the past 10 years as a promising technology for energy generation and wastewater treatment. A MFC is different from a conventional chemical fuel cell. In a typical MFC, the bacteria oxidize a substrate (sugars, acetate or organics) in the absence of oxygen to generate electrons which are then transferred to the electrode. The main distinction between bio-batteries and microbial fuel cells is that microbial fuel cells have their substrate refilled either continuously while the bio-batteries operate in batch mode (Logan *et al.*, 2006). For long term operations, continuous MFCs are used with substrate fed continuously to investigate the evolution of microbial community and electrochemical characteristics. Usually, air cathodes or chemical cathodes are used with a precious metal catalyst like platinum. In air cathodes, the metal catalysts help in reducing oxygen effectively, while the chemical cathodes rely on reversible chemical oxidizing agents such as potassium ferricyanide. The ferricyanide based cathodes produce 1.5 to 1.8 times increased power density over conventional platinum covered cathodes using dissolved oxygen (Oh and Logan, 2006). The low redox potential of the anaerobic anode and the high redox potential of the aerobic or chemical (ferricyanide) cathode is the driving force for the transport of electrons.

A proton exchange membrane separates the anode and cathode chambers. The proton exchange membrane allows the transport of positively charged ions (protons) from the anode to

the cathode, thereby maintaining pH and electro-neutrality. Salt bridges or ionic conductive separators can also be employed, but these separators affect the fuel cell performance due to high Ohmic resistance contribution (Min *et al.*, 2005). The conventional MFC design is an 'H' type dual chamber design containing two bottles separated by a tube containing the proton exchange membrane like Nafion^{tm}. These MFCs are used for basic research, such as examining the performance of new electrode materials and produce lower power densities compared to single chamber MFCs due to high internal resistance (Logan, 2006). A single chamber MFC design, where the proton exchange membrane is either removed or pressed against the anode or cathode to form Membrane Electrode Assemblies (MEAs) produce increased power generation by decreasing the internal resistance.

A few species of bacteria have the ability to transfer electrons without electron mediators. They transfer electrons through conductive nanowires when grown as a bio-film on the electrode surface and are called as exoelectrogenic bacteria. Electron mediators are required by non-exoelectrogenic bacteria that cannot transfer electrons from their cells to the electrodes. These mediator compounds have the ability to penetrate into the cells of these non-exoelectrogenic bacteria, react with the NADH molecules within the bacterial cells and exit the cells in the reduced form, thereby transferring the electrons to the electrode.

2.2 Electrodes

Electrodes play a vital role in the performance and cost factors of MFCs as they improve bacterial adhesion and electron transfer. Several factors should be considered when using these electrodes including bio-compatibility, conductivity, surface morphologies and properties, cost and modification methods. Generally, an ideal electrode must have good conduction, chemical stability, high mechanical strength, low cost, scalability and corrosion resistance. These

electrodes must provide a large surface area for bacterial adhesion and current generation (Wei *et al.*, 2011).

2.2.1 Carbonaceous electrodes

Carbonaceous materials are widely employed owing to their good bio compatibility, chemical stability, low cost and high conductivity. He and colleagues used reticulated vitreous carbon electrodes that produced a maximum power density of 170 mW/m^2 (He *et al.*, 2005). Plane carbon paper electrodes of 22.5 cm^2 have also been also used yielding a maximum power density of 600 mW/m^2 (Wei *et al.*, 2011). Aelterman *et al*. (2008) worked with graphite felt and carbon felt to achieve power densities of 386 W/m^3 and 356 W/m^3 (anode volumes) respectively. Carbon mesh have also been examined as an inexpensive alternative to carbon paper and carbon cloth (Wang *et al.*, 2009). While carbon cloth electrodes are physically flexible and offer high surface areas, they are expensive to use in MFCs (Zhang *et al.*, 2010). A graphite brush anode was first used by Logan *et al.* (2007) and it has high surface area, high porosity, and efficient current collection. These graphite brush anodes produced a maximum power density of 1430 mW/m^2, versus 600 mW/m^2 generated by plain carbon paper anodes (Logan *et al.*, 2007).

2.2.2 Metal electrodes

Noble metal electrodes such as platinum, gold etc. are quite rare and expensive. Stainless steel is a cheaper and corrosion resistant alternative. However, stainless steel electrodes have not been studied as extensively as the carbonaceous electrodes and have only been showed to work as cathodes (Zhang *et al.*, 2010) and under marine conditions in seafloor microbial fuel cells; these fuel cells were driven by the potential difference between anaerobic and aerobic regions of the sea bed and the sea surface respectively (Dumas *et al.*, 2007). Dumas *et al.*, (2008a) found that the stainless steel anode based fuel cell produced lower power than a graphite one. In

contrast, Erable and Bergel (2009) found that under a constant potential (−0.1 V_{SCE}), a stainless steel grid anode produced much higher current densities than plain graphite ones. In another study nitrogen doped carbon nanofibres (NCNFs) were grown on stainless steel mesh electrodes which formed a water resistant and binder free cathode in addition to providing a large surface area for microbial adhesion (Chen *et al.*, 2012).

2.2.3 Surface coating of electrodes

Immobilization of mediators on the electrode surface has been attempted to improve the performance of fuel cells. Park *et al.* (2003) immobilized Mn^{4+} and Fe^{3+} on graphite electrodes and noted significantly improved electron transport. Methylene blue immobilized on stainless steel electrodes were found to perform well in photosynthetic biocathodes, compared to soluble mediators (Godwin, 2011). Polyaniline and polypyrrole are electrically conductive and have also been used to improve the performance of the fuel cells (Qiao *et al.*, 2007).

2.2.4 Carbon nanoparticles and nanotubes

The structural chemical and electrical properties of carbon nanoparticles and carbon nanotubes have paved way for the development of unique and efficient electrode materials (Fan *et al.*, 2011). Microbial fuel cells containing pure cultures of *Proteus vulgaris* entrapped on carbon cloth electrodes using carbon nanoparticles and PTFE were used under mediator (Yuan *et al.*, 2009) and mediatorless (Yuan *et al.*, 2011) setups that produced power densities of 706 mW/m^2 and 260 mW/m^2 respectively. Gold and palladium nanoparticle decorated graphite anodes produced a 20-fold increase in the power output compared to plain graphite. However, the power output was greatly dependent on the size and shape (circularity) of the nanoparticles (Fan *et al.*, 2011). Pt/Ni supported on Multi Walled Carbon Nanotubes (MWCNTs) were compared with conventional Pt/C cathodes and found to be promising electrodes for oxygen

reduction at the cathode in terms of cost and coulombic efficiency (Yan *et al.*, 2013). Titanium oxide decorated CNTs were used as anode electrodes in a dual chambered fuel cell setup and they were found to significantly improve the performance of the fuel cell, confirmed through Electrochemical Impedance Spectroscopy analyses (Wen *et al.*, 2013).

2.3 Mediators

Mediators act as electron shuttles and aid in the transfer of electrons to the electrode surface. These electron shuttles are stable in their reduced and oxidized states, do not biologically degrade and are generally non-toxic towards microorganisms (Park *et al.*, 2003). Moreover, these mediators in their oxidized states have the ability to penetrate into cells, react with the NADH molecules present in the microbes and leave the cells in their reduced state, thereby passing electrons to the anode (Powell *et al.*, 2009). Some of the commonly used mediators are methylene blue (Godwin, 2011), neutral red (Wang *et al.*, 2009), thionin (Yuan *et al.*, 2009),2-hydroxy-p-napthaquinone (Powell *et al.*, 2011), polyviologen (Kim *et al.*, 2011), Anthraquinone-2,6-disulfonate (Ringeisen *et al.*, 2006), of which poly(methylene blue) received much of the attention owing to its high stability and favorable reversible potential (Karyakin *et al.*, 1999). Most of these mediator compounds have been proven to maintain their redox property even after electropolymerization on an electrode (Karyakin *et al.*, 1999; Prieto-Simón *et al.*, 2004). Research works involving immobilization of mediator and nanoparticles/nanotubes to enhance the surface area have also benn done (Qiao *et al*., 2007; Scott *et al*., 2007). These immobilized mediators aid the non-exoelectrogenic microorganism in transferring the electrons to the anode (Park and Zeikus, 2003). Enzyme based bio-sensors use polymer redox compounds as solid surface electron mediators (Silber *et al.*, 1996). In fact, some redox polymers such as polyaniline and polypyrrole are conductive and aid in electron transport, thereby partially

eliminating the need for mediators (Godwin, 2011). Polypyrrole was used by researchers as a conductive polymer, which was polymerized on non-noble metals providing an oxidation blocking barrier for metals (Martins *et al.*, 2004). Figure 2.1 and Figure 2.2 represents the conductive (oxidized) form of polyprrole and poly (methylene blue) with monomers attached to their nitrogen groups respectively.

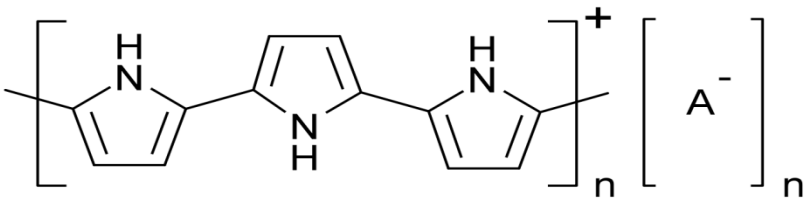

Figure 2.1 Conductive (oxidized) form of polypyrrole doped with an anion denoted by A^- (Vernitskaya and Efimov, 1997).

Doping ions can be used to prevent the oxidation of metals and increase the conductivity of polymer films. Some of the commonly used ions for this purpose include malate, oxalate (Martins, 2004) and salicylate (Petitjean, 1999) among which salicylate was found to perform better (Godwin, 2011).

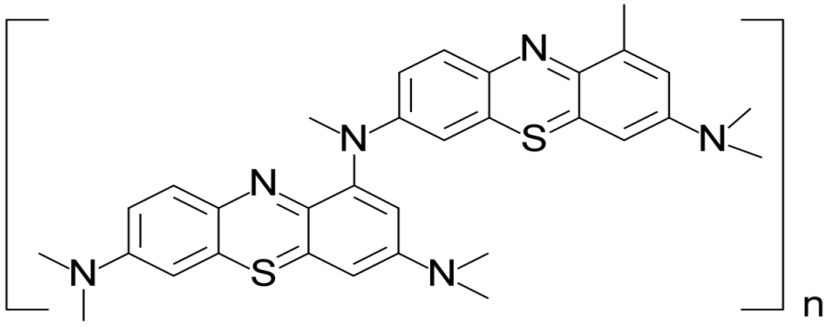

Figure 2.2 Structure of poly methylene blue (Karyakin *et al.*, 1999).

2.4 Substrates

The substrate added to the MFC also plays a crucial role as the maximum theoretical voltage of the fuel cell is dependent on the substrate concentration. Several substrates from simple sugars to synthetic wastewater have been used in biological fuel cells. Glucose and acetate are the most commonly used substrates when high electrical performance is desired and aspects other than microbial growth are being studied. The theoretical potential of the anode with respect to a standard hydrogen scale is calculated from the Gibbs free energy formula as follows (Godwin, 2011):

$$\mathbf{Eo} = -{}^{\Delta \mathbf{G}}/_{\mathbf{nF}} \qquad \mathbf{(2.1)}$$

Using the Nernst equation the theoretical potential at non-standard conditions can be determined:

$$\mathbf{E} = \left(-{}^{\Delta \mathbf{G}}/_{\mathbf{nF}}\right) - {}^{\mathbf{RT}}/_{\mathbf{nF}} \ \mathbf{ln}\ (\mathbf{\Pi}) \qquad \mathbf{(2.2)}$$

Table 2.1 lists the commonly used electron donors and acceptors in anodes and cathodes of biological fuel cells.

Table 2.1 Some common electron donors and acceptors used in MFCs

CHAMBER	ELECTRON DONOR/ACCEPTOR
ANODE	Acetate Glucose Butyrate Glycerol Malate Citrate Sulfur
CATHODE	Oxygen Bicarbonate Acetate Nitrate Nitrite Permanganate Manganese dioxide Iron Copper (II) Potassium persulfate Ferricyanide

2.5 Biocathodes and photosynthetic cathodes

Conventional MFCs consist of biological anode and chemical cathode. Chemical cathodes are enhanced when a metal catalyst such as platinum is incorporated to enhance the oxygen reduction reaction. However, these metal catalysts are expensive and cause secondary contamination. Biocathode MFCs using microorganisms are helpful in lowering cost and improving sustainability. Moreover, they are economical and environment friendly.

In a recent student cathodic bio-films formed on graphite electrodes achieved a fourfold increase in current output compared to non-catalyzed graphite cathodes (Freguia *et al.*, 2008). A biocathode MFC catalyzed by ferro/manganese-oxidizing bacteria was investigated by Mao *et al.* (2010) and produced a maximum power output of 32 W/m^3 and 28 W/m^3 for fed batch and continuous systems respectively. Photosynthetic biocathodes using microalgae *Chlorella vulgaris* to reduce carbon dioxide were investigated by Powell *et al.* (2011). Two mediator compounds were tested: methylene blue and 2-hydroxy-p-naphthaquinone (HNQ). When these mediators were dissolved in the cathode, the growth rate of the microalgae was lower in the presence of methylene blue than HNQ. This phenomenon could be attributed reduction in illumination intensity caused by the methylene blue. *Chlorella vulgaris* based cathodes were also used in a mediatorless setup to treat the wastewater in anodic chamber and has been reported to produce electricity during the dark phase (at night) (González del Campo *et al.*, 2013). Moreover, bacterial biofilms have been found to catalyze oxygen reduction at the cathode by utilizing the electrons transferred from the anode (Logan, 2009).

2.6 Electrochemical/electroanalytical techniques

Potential sweeps, cyclic voltammetry and EIS are the commonly used electrochemical techniques. Researchers use potential sweeps to generate the polarization (voltage-current)

curves and it has been shown that the maximum power output is obtained when the internal resistance (R_{int}) of the cell is equal to the external resistance (R_{ext}) (Manohar and Mansfeld, 2009). Cyclic voltammetry is a tool that's used for the synthesis of compounds on electrodes. Cyclic voltammetry is also used for measuring electrode kinetics in irreversible systems and is used extensively in the analysis of microbial fuel cells (Manohar *et al.*, 2009; Schröder *et al.*, 2003; Logan *et al.*, 2006). In MFCs and bio-batteries, Cyclic voltammetry (CV) is used to analyze the electrochemical activity of the microbial cultures in the anolyte and also to provide insight into the mechanism of direct electron transfer from bio-film to the electrode. MFC studies employing CV generally have scan rates ranging between 0.1 and 100 mV/s and the peaks on the CV plot indicate the redox species present in the electrochemical system. Electrochemical Impedance Spectroscopy (EIS) is a technique that provides a wealth of information such as electrolyte and electrode conductivities, determination of kinetic parameters, bio-film behaviour and reaction mechanisms. In MFCs and bio-batteries, EIS is generally used to determine the elements in the system that control the rate of reaction.

2.6.1 Chronopotentiometry

Chronopotentiometry is a galvanostatic method and in this method, the potential is measured while maintaining a constant current over a particular time interval. Conductive polymers such as pyrrole can be formed on the surface of an electrode by applying anodic current or potential. Often a counter ion such as salicylate that forms an insoluble compound with the base metal is added and a constant current is supplied. Metal dissolution occurs until this metal-salicylate layer is formed on the electrode. Then polypyrrole begins to form on the surface of the electrode at a much higher potential than metal dissolution (Godwin, 2011).

Air cathodes coated with polytetrafluoroethylene (PTFE) have been studied using this technique, where the electrode potentials of the layered carbon cloth electrodes were measured whilst applying a constant current. The electrode performances were then evaluated by plotting the resulting potentials as a function of current density (Cheng *et al.*, 2006).

2.6.2 Cyclic voltammetry (CV)

Cyclic Voltammetry (CV) is a technique frequently used for the determination of the electrode reaction mechanisms occurring in the fuel cell chambers. Cyclic voltammetry is also used for the polymerization of exogenous mediators (methylene blue) on metal electrodes (Godwin, 2011). In biological fuel cell studies, CV experiments have been used extensively to: (i) investigate the mechanisms of electron transfer (both direct and indirect) between the bio-film and the electrode; (ii) evaluate the performance of catalysts; and (iii) to determine the redox potentials of the chemical or biological species involved undergoing electrochemical reactions. Cyclic voltammetry is a simple technique that produces results in a relatively short time. The cyclic voltammogram depend on several factors, such as the electrode pretreatment, the rate of the reactions (electron transfer), the thermodynamic properties of the chemical and biological species present, the concentration and rates of diffusion of electroactive species and the sweep rate.

2.7 MFC performance analysis

Several electrochemical methods have been used by researchers to study the performance of the MFCs. Slow potential sweeps have been used to generate the polarization curves (Hoffman *et al.*, 2013; Schroder *et al.*, 2003) and determine the maximum power output of the cell (Logan *et al.*, 2006). Cyclic voltammetry plots have been used to study the electrochemical activity attributed to microbial metabolism and the interaction of the bio-film with electrodes

(Manohar *et al.*, 2009; Logan *et al.*, 2006). Electrochemical Impedance Spectroscopy (EIS) is a powerful tool that is used to study the internal resistance components (Manohar and Mansfeld, 2009). By fitting the EIS impedance data to equivalent circuits, the solution resistance, charge transfer resistance and double layer capacitance can be determined along with the individual polarization resistances of each half cell (Manohar *et al.*, 2008). Differential pulse voltammetry has been proposed for systems that take a long time to reach pseudo-steady state potentials. However, there is no evidence of the use of differential pulse voltammetry for characterizing MFCs in the literature.

2.7.1 Polarization and power curves

Polarization curves help in expressing the performance potential of microbial fuel cells and bio-batteries through the measurement of open circuit voltages and voltage-current behavior. There are four methods of determining polarization curves: a) Constant resistance discharge methods by connecting different resistors to the bio-battery and recording the current and voltage output; b) Polarization sweep methods like Linear Sweep Voltammetry (LSV) conducted at a slow scan rate (i.e., 0.1 or 0.15 mV/s); c) Galvanostatic discharge methods like chronopotentiometry where the current is kept constant and the resulting voltage is measured and d) Potentiostatic discharge methods where the potential is controlled and the resulting current is measured.

An ideal polarization curve recorded for a MFC is shown in Figure 2.3 and it illustrates three characteristic regions.

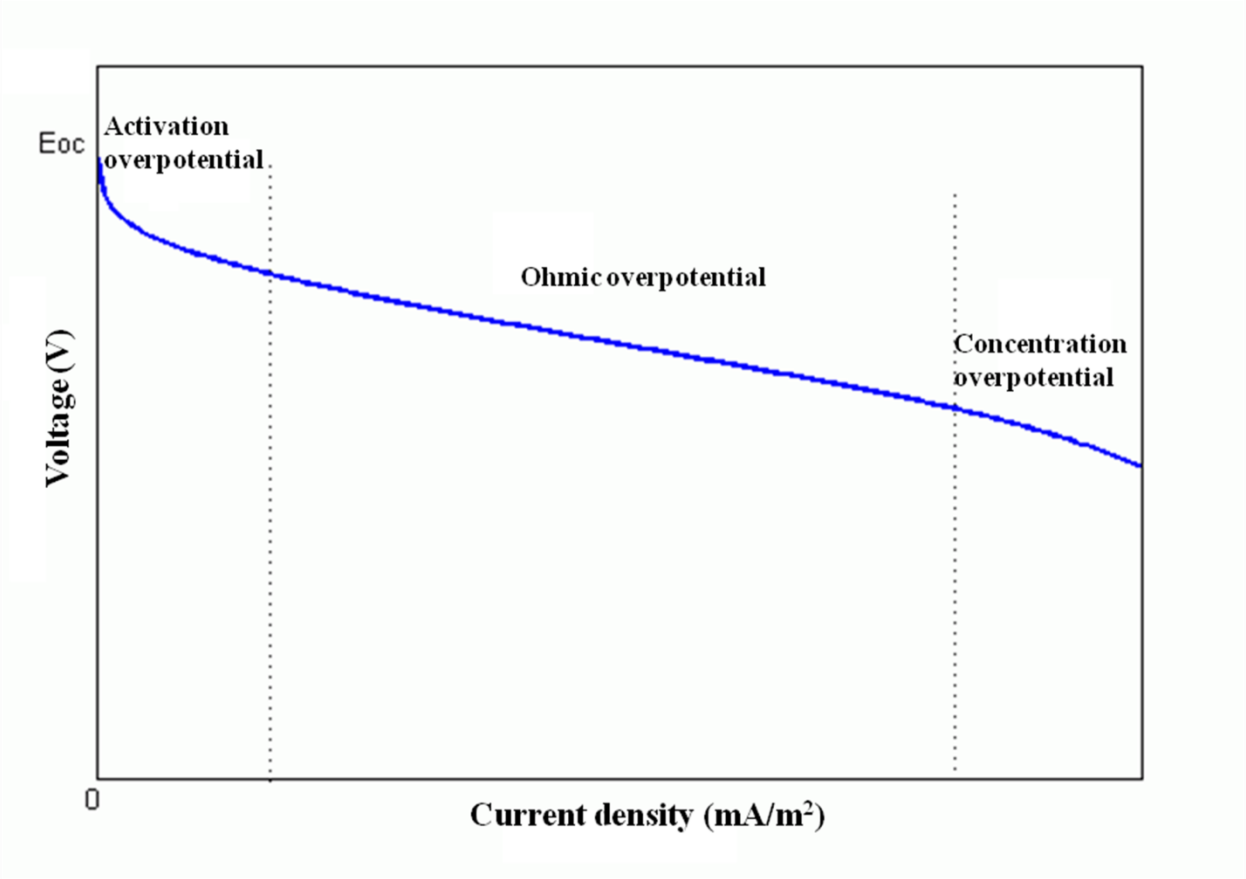

Figure 2.3 Example of a polarization curve for MFCs and bio-batteries.

These three regions are usually overlapped for MFCs and biobatteries, while they are well segregated in chemical fuel cells. The region at low current densities represents charge transfer (activation) overpotential corresponding to the rate of the reactions taking place on the surface of the electrodes. Electrode materials, catalysts and reactants, electrolyte and mediators, metabolism of microorganism and bio-film characteristics are some of the common factors that influence charge transfer overpotentials.

The intermediate region of the polarization curve represents the Ohmic overpotential. The ohmic overpotential is caused primarily by solution resistance, ionic concentration changes and the membrane.

The final region at high current values represents the mass transfer (concentration) overpotential. This overpotential results from the changes in the concentration of the reactants at the interface between the electrode surface and the bulk electrolyte. This overpotential occurs when the reactants cannot be supplied to the electrode surface reaction sites at the rate faster than they are being depleted. The major factor affecting mass transfer overpotential are the transport properties of the electroactive species with an indirect influence of the hydrodynamics in the bulk solution.

2.7.2 Electrochemical Impedance Spectroscopy

Electrochemical Impedance Spectroscopy (EIS) tests helps determining the electrochemical characteristics of the system. Some examples of these are: coating coverage; solution resistance; charge transfer resisance and; double layer capacitance (Manohar *et al.*, 2008). Subsequently, the membrane resistance can be calculated using Ohm's law (Manohar and Mansfeld, 2009). EIS is frequently used for studying corrosion processes and evaluate corrosion protection by polymer coatings and inhibitors. Recently EIS was used for determining the internal resistances involved in MFCs (Manohar *et al.*, 2008). EIS experiments are conducted either at fixed potentials or open circuit potentials (He and Mansfeld, 2009). Generally, phosphate or carbonate buffers as supporting electrolytes (Fan *et al.*, 2008). However, the membrane contributes to a large extent of the ohmic resistance in a two chambered microbial fuel cell. In EIS, a sinusoidal voltage of varying frequency is applied to the working electrode producing an impedance spectrum. These small sinusoidal perturbations prevent the interference of non-harmonic effects on data collection and prevent damage to the bio-films attached on the electrodes.

There are two methods of visualizing the spectrum, a) Nyquist plot and b) Bodé plot. The Nyquist method plots the imaginary portion versus the real portion of impedance. Nyquist plots

are useful in determining the resistances and characterizing the physical processes occurring in the system. However, since the frequency is not clearly shown (since it is a polar plot), time dependant parameters cannot be identified. Bodé plots on the other hand, are used for representing all the three values i.e., impedance, phase angle and frequency. Frequency is plotted along the abscissa while the phase angle and magnitude are plotted along the ordinate axis. The impedance data is usually fit to an electrical equivalent circuit for estimating the resistance and capacitance.

The simplest circuit used to model an electrochemical system is the Randles cell. The Randles cell contains a resistor (due to solution and electrode resistance) in series with a parallel combination of a capacitor and resistor. This parallel combination represents the charge transfer resistance between the electrolyte and electrode and also the double layer capacitance. Usually, the double layer capacitance is replaced with a constant phase element (CPE) due to non-homogeneity (non uniform surface properties or concentrations) of the electrodes. The true capacitance is represented as $C = Q\omega^{n}_{max}$, where ω_{max} is the frequency at which the imaginary component of the impedance is maximum and Q (in units $S.s^{n}$) is analogous to C (in units S.s) (Godwin, 2011).

The mass transfer overpotential or concentration overpotential is caused by the concentration gradient created near the electrode by the limited diffusion rate of the reactants. The Warburg impedance is used to describe the diffusion effects taking place in an electrochemical system and represents semi infinite diffusion within the electrolyte. A Warburg impedance has a magnitude of $\sqrt{2}\sigma/\omega^{1/2}$ (σ is the Warburg constant) and is at a constant phase angle of 45^{o}, regardless of frequency. In some particular cases, like the rotating disk electrode and electrode coating experiments, the diffusion layer thickness is finite and a special impedance

element called ‘porous bounded Warburg’ or ‘O element’ is used. The porous Warburg impedance is similar to Warburg impedance at high frequencies, but at low frequencies, the imaginary component of the impedance approaches zero.

2.8 Challenges and knowledge gap

The primary challenge faced in the development of biological fuel cells is the low power output caused, to some extent, by high internal resistance within the system. Dual chambered biological fuel cells are plagued by high ohmic and activation resistances (Manohar *et al*., 2008). In addition, the power output of biological fuel cells are lower than conventional chemical fuel cells due, in large part, to microbial metabolism. In order to counter the slow electron transport rate, exogenous mediators have been used to shuttle the electrons from inside to outside the cells. However, these exogenous mediators must be replenished often and are known to cause solution contamination. Immobilizing them directly on the electrode surfaces can reduce these problems.

Microbial fuel cells generally rely on bio-films formed on the electrode surface to generate a steady power output. These bio-films usually take a long time to be formed. The concept of bacteria immobilization directly on the anode surface was studied by Yuan *et al*., 2009 and this concept was found to reduce the start up time of the fuel cell compared to a conventional bio-film based one.

It is hypothesized in this research that mediator and bacteria immobilization directly on the electrode surface will enhance the electron transfer rate from the bacterial cells to the electrode, by reducing mass transfer and/or electrochemical resistances. In addition, the use of carbon nanoparticles will increase both the surface area and enhance the conductivity of the electrode, thereby improving the performance of the battery.

3. MATERIALS AND METHODS

This chapter includes a detailed description of the equipment and various experimental methodologies adopted in this research. The first few sections of this chapter contain details about preparation and testing of the composite electrodes, followed by a description of the bacteria immobilization technique using CNP and Teflon[tm], substrate concentration analysis, bioanode, biocathode and complete bio-batteries setup and analyses.

3.1 Electrochemical Equipment

A Gamry[tm] Reference 600 potentiostat along with PHE 200[tm] software was used for electro-polymerization of pyrrole and mediator (methylene blue), measuring open circuit potentials, and obtaining polarization curves. A Gamry[tm] Interface 1000 potentiostat was used for the Electrochemical Impedance Spectroscopy (EIS) analysis with the data being fit using equivalent circuit models. The Gamry[tm] Echem Analyst software was used to design and fit equivalent circuit models to EIS data and also to export the data to Microsoft Excel[tm] for calculations and plotting. These programs were operated from within the Gamry[tm] Framework 6.0 software. The potentiostats were calibrated using a standard cell in a Faraday's cage prior to running experiments. Hanna instruments stir plates were used for stirring the solutions. Figure 3.1 shows the Gamry[tm] Interface 1000 and Reference 600 potentiostats.

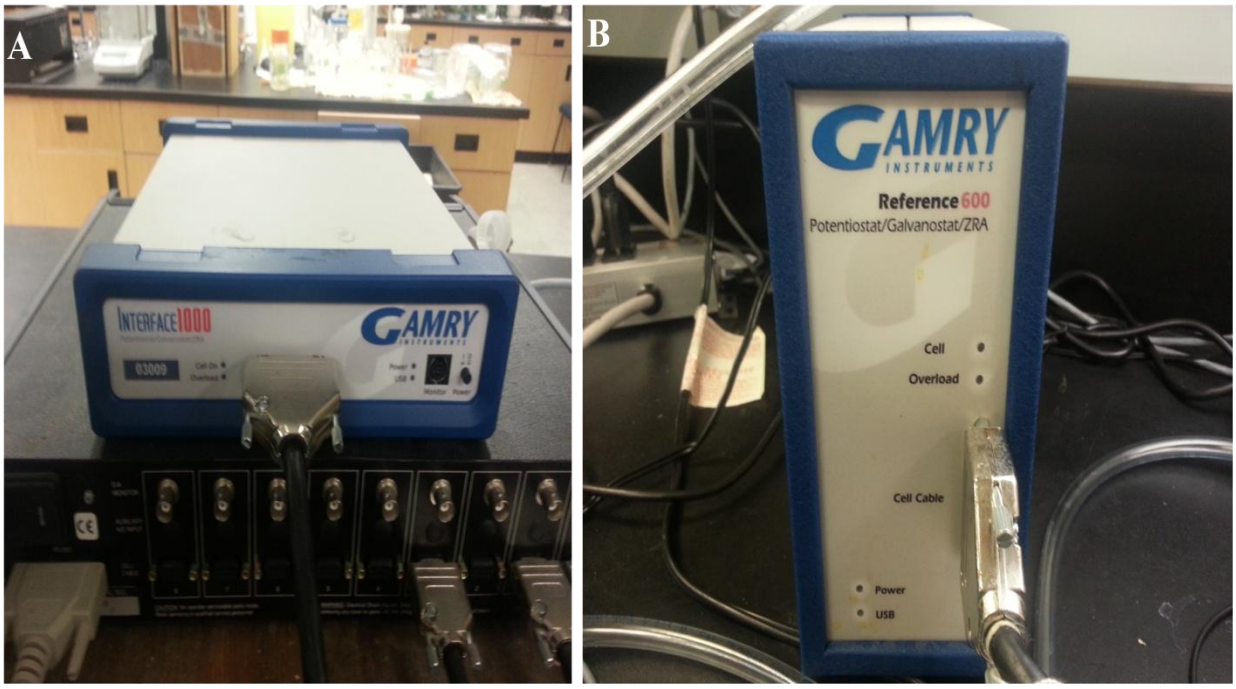

Figure 3.1 Gamry[tm] Potentiostats A) Interface 1000 for EIS analysis and B) Reference 600 for electropolymerization and obtaining OCP and polarization curves.

3.2 Electrode design and preparation

Composite electrodes were prepared with stainless steel mesh as the base and by polymerizing pyrrole and methylene blue (mediator) on the base. These composite electrodes were then coated with the CNP-bacteria paste prepared using Teflon[tm].

3.2.1 Composite electrode preparation

Stainless steel mesh (60x60) and 2.54 cm diameter was obtained from McMaster-Carr, Canada. The mesh was washed with acetone to remove any metal fragments that may interfere with polymerization. The method used for electro-polymerization of pyrrole and mediator on the mesh was similar to the method used by (Godwin and Evitts, 2011) with a slight variation in solution concentration due to the geometry and morphology of stainless steel mesh.

Polymerization of pyrrole on the stainless steel mesh electrodes was conducted galvanostatically (chronopotentiometry experiment) in a three electrode cell, at a current density of 6 mA/m^2. The three electrode cell used is shown in Figure 3.2. It consisted of the working electrode, graphite counter electrode and saturated calomel reference electrode. The solution contained 0.350 mol/L pyrrole, 0.080 mol/L salicylate and small amounts of orthophosphoric acid to bring the pH down to 4.2. The polymerization time was approximately 180 seconds.

Subsequently, cyclic voltammetry was used for the polymerization of methylene blue on the polypyrrole coated stainless steel mesh. The solution used for methylene blue polymerization was 0.001 mol/L methylene blue, 0.1 mol/L potassium nitrate, 0.025 mol/L sodium borate, and pH of 9.5. The electrode setup for methylene blue polymerization was similar to Figure 3.2. The methylene blue dye was polymerized on the surface of polypyrrole coated stainless steel mesh by ten cyclic voltammetry sweeps between -0.4 and 1.05 V.

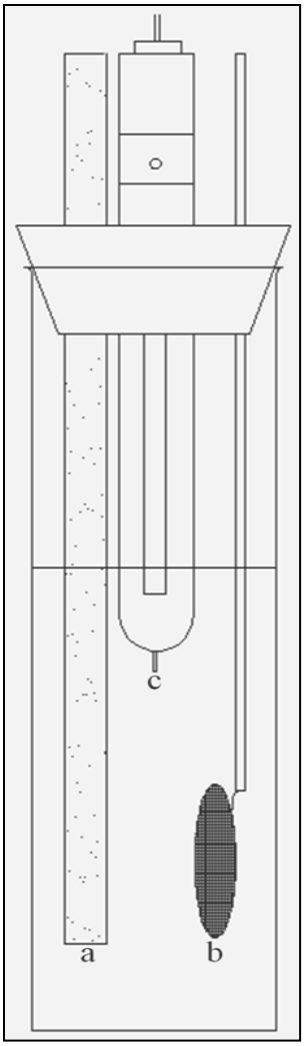

Figure 3.2 Schematic representation of the three electrode cell for polymerization of pyrrole and methylene blue: a) graphite counter electrode b) stainless steel mesh working electrode and c) saturated calomel reference electrode.

3.2.2 Bacteria-Carbon paste coating preparation

The methodology for bacteria immobilization on the composite electrode was modified from the method used by Yuan *et al.* (2011). In this method, 0.3 g of Vulcan XC-72 R (carbon nanoparticles) was homogeneously spread in 10 mL of water using ultrasonication. The bacteria (*Escherichia coli K-12),* was a pure culture obtained from the American Type Culture Collection

(ATCC^{tm} 29425^{tm}). The cultures were grown aerobically in Erlenmeyer flasks placed in a shaker set at 37°C and 250 rpm for 24 hours. The medium used for the growth contained: 10.00 g/L of tryptone, 10.00 g/L of NaCl, 5.00 g/L of yeast extract and 20.00 g/L of glucose. The medium was sterilized in an autoclave before culturing the bacteria. The cultured bacteria were harvested from the liquid culture through centrifugal action (8000 rpm for 10 minutes) and introduced into the container containing carbon particles. This solution was stirred for 2 minutes and 1 mL of Teflon^{tm} emulsion (Teflon, PTFE 3859, DuPont, USA) containing 60% (by weight) resin in water was mixed with the carbon nanoparticles to form the Carbon Nanoparticle and bacteria paste (CNP-bacteria paste). The final solution was stirred for at least 2 minutes until a sticky CNP-bacteria suspension was obtained which was then evenly applied on both the sides of the composite mesh electrode. Figure 3.3 shows the final composite electrode after bacteria immobilization.

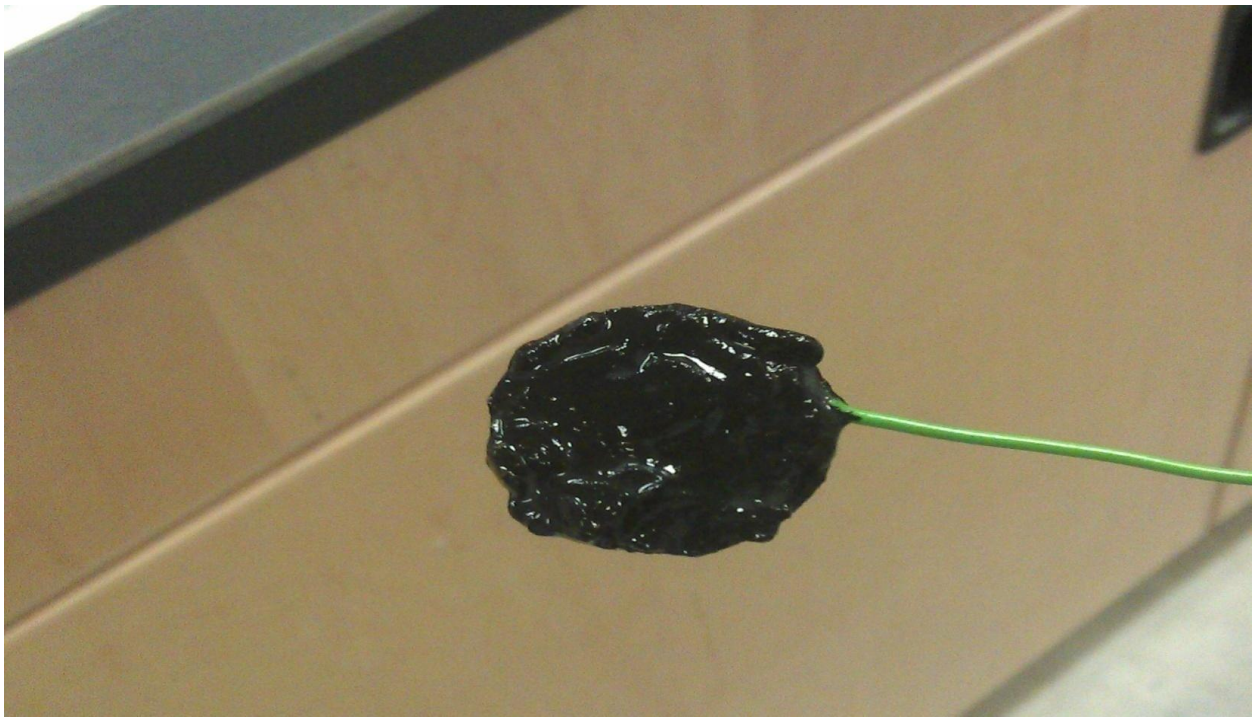

Figure 3.3 Final composite electrode with CNP-bacteria paste coating.

3.3 Electrode setup

Different electrode configurations and setups were used for bioanodes, biocathodes and complete bio-battery experiments.

3.3.1 Bacteria culture and bioanode setup

Figure 3.4 shows the H-type configuration of the fuel cell with bioanode, where both the anode and cathode chambers had a capacity of 600 mL each. Both of the chambers were filled with 500 mL of solution and separated with a Nafion^{tm} proton exchange membrane with an approximate surface area of 5 cm^2. The Nafion^{tm} 117 membrane (supplied by Sigma-Aldrich) was pre-treated by boiling for 1 hour in each of two solutions: 3% H_2O_2 de-ionized water and 0.5 M H_2SO_4. Pre-treatment of Nafion^{tm} membranes is essential to receive high power density and coulombic efficiency in dual chambered MFCs (Ghasemi *et al.*, 2012) . For the bioanode experiments, the anode chamber contained L-B medium with buffer solution (10 g/L sodium bicarbonate, 8.5 g/L potassium di-hydrogen phosphate) and 20 g/L glucose at a pH of approximately 6.5. Sterile graphite and saturated calomel reference electrodes were inserted into the cathode chamber while the composite mesh electrodes covered with CNP-bacteria paste were inserted into the anode chamber. Nitrogen was purged into the anode chamber in order to maintain anaerobic conditions and the setup was run at an ambient room temperature of 22°C. Magnetic stirrers were used throughout the experiment in both the chambers to induce mixing and maintain a uniform composition.

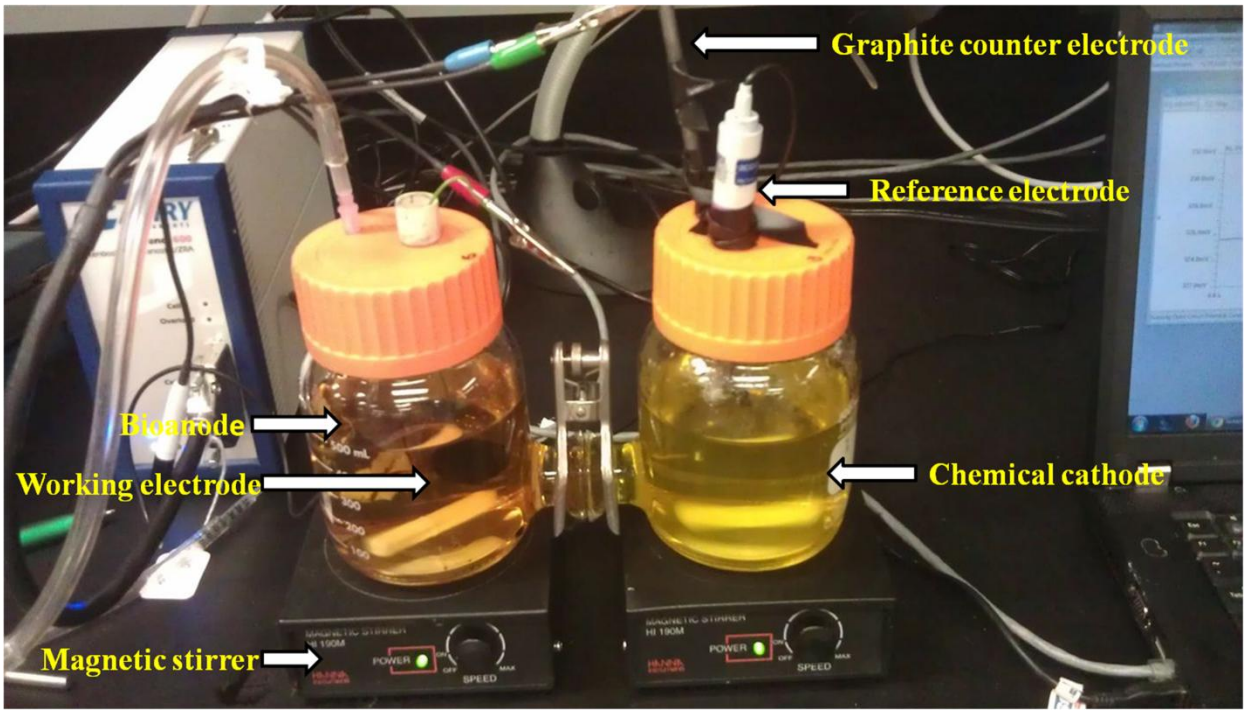

Figure 3.4 Fuel Cell apparatus containing the composite electrode with CNP-bacteria paste coating. The cathode contains 100 mM potassium ferricyanide solution with graphite electrode.

The composite electrode with CNP-bacteria coating was compared with two other electrode configurations. These alternate configurations include: Case I, a composite electrode with CNP paste coating and bacteria suspended in solution, and Case II, a composite electrode with bacteria suspended in solution. The CNP paste coating for Case I was prepared by homogeneously spreading 0.3 g of CNP in 10 mL of water by ultrasonication and adding 1 mL of Teflon^{tm} to the carbon nanoparticle suspension.

3.3.2 Algae culture and photosynthetic biocathode setup

Chlorella vulgaris and *Scenedesmus sp*. were obtained from Carolina Biological Supply, Burlington, NC and were stored in a refrigerator until used. Starter cultures of *Chlorella vulgaris*

and *Scenedesmus sp.* were initially grown in flasks containing Alga-Gro^{tm} fresh water medium (obtained from Carolina Biological Supply, Burlington, NC) for at least one week. The starter cultures were grown under plant growth lights that had a light intensity of approximately 4000 lx and timers were used to control the lights to be on for 16 hours a day. Magnetic stirrers were used to prevent the cells from precipitating. For the starter cultures, no CO_2 supplementation was provided or other gasses blown into the flasks.

Biocathodes were tested using 20 mM ferrocyanide as the electron donor in the anode in a similar H-type configuration used for bioanode batteries. Figure 3.5 shows the biocathode battery setup with a chemical ferrocyanide anode. Approximately 500 mL of Bold's medium was added to the cathode chamber and inoculated with approximately 50 mL of starter algae culture. The contents of the medium are shown in Table 3.1.

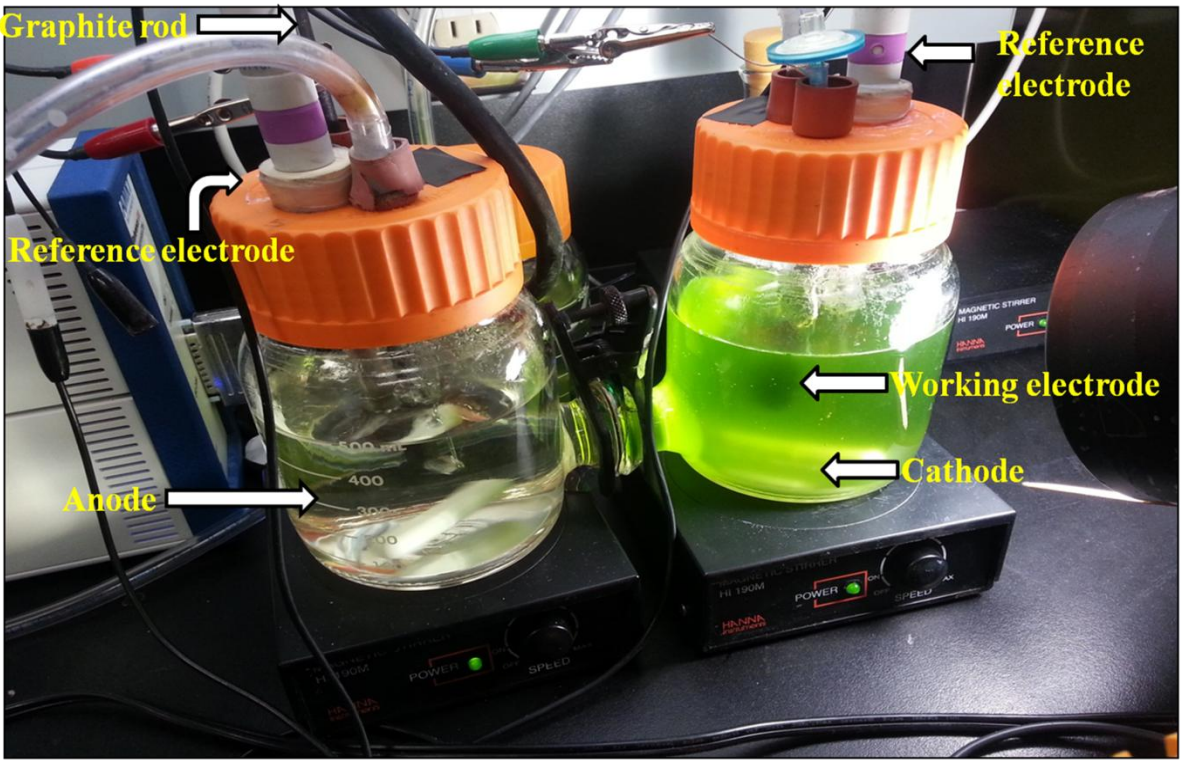

Figure 3.5 Fuel setup with the biocathode with a 20 mM ferrocyanide anode.

Table 3.1 Bold's basic medium minerals and nutrients

Nutrients	Conc. (mg/L)
NH_4Cl	75
$MgSO_4 \cdot 7H_2O$	50
K_2HPO_4	100
KH_2PO_4	150
$CaCl_2$	25
NaCl	25
Na·EDTA	50
Trace Elements	
$FeSO_4 \cdot 7H_2O$	4.98
H_3BO_3	11.42
$ZnSO_4$	8.82
MoO_3	0.71
$Co(NO_3)_2 \cdot 6H_2O$	0.49
$MnCl_2$	1.44
$CuSO_4 \cdot 5H_2O$	1.57

Pre-calibrated gas flow meters were used to mix CO_2 and air. Eight percent CO_2 was mixed with air and introduced into the cathode chamber at a flow rate of 200 mL/min. Graphite rods served as the counter electrode in the anode while the composite electrode configurations were

used as the working electrodes in the cathode. Two different composite electrode configurations were tested: 1) Composite electrode with CNP coating (prepared using carbon nanoparticles and Teflon^{tm}) and 2) composite electrode without CNP coating. Tests were conducted with respect to the reference electrode placed in the chemical anode due to the unstable nature of ferrocyanide.

3.3.3 Complete bio-battery setup

The complete bio-battery setup combined the bioanode containing bacteria and the biocathode containing algae as shown in Figure 3.6. The anode contained composite electrode with CNP-bacteria paste while the cathode had composite electrode with carbon paste coating and *Chlorella vulgaris* suspended in the solution. The anolyte was LB-Miller medium with bicarbonate buffer with a pH of approximately 7.0 and the catholyte was Bold's Basic medium. Due to the pH drop caused by CO_2 in the cathode chamber, the pH of the catholyte was maintained between 6 and 7 by adding small amounts of sodium bicarbonate solution. Reference electrodes were introduced in both the chambers and magnetic stirrers were used throughout the experiment to prevent settling and maintain uniform composition.

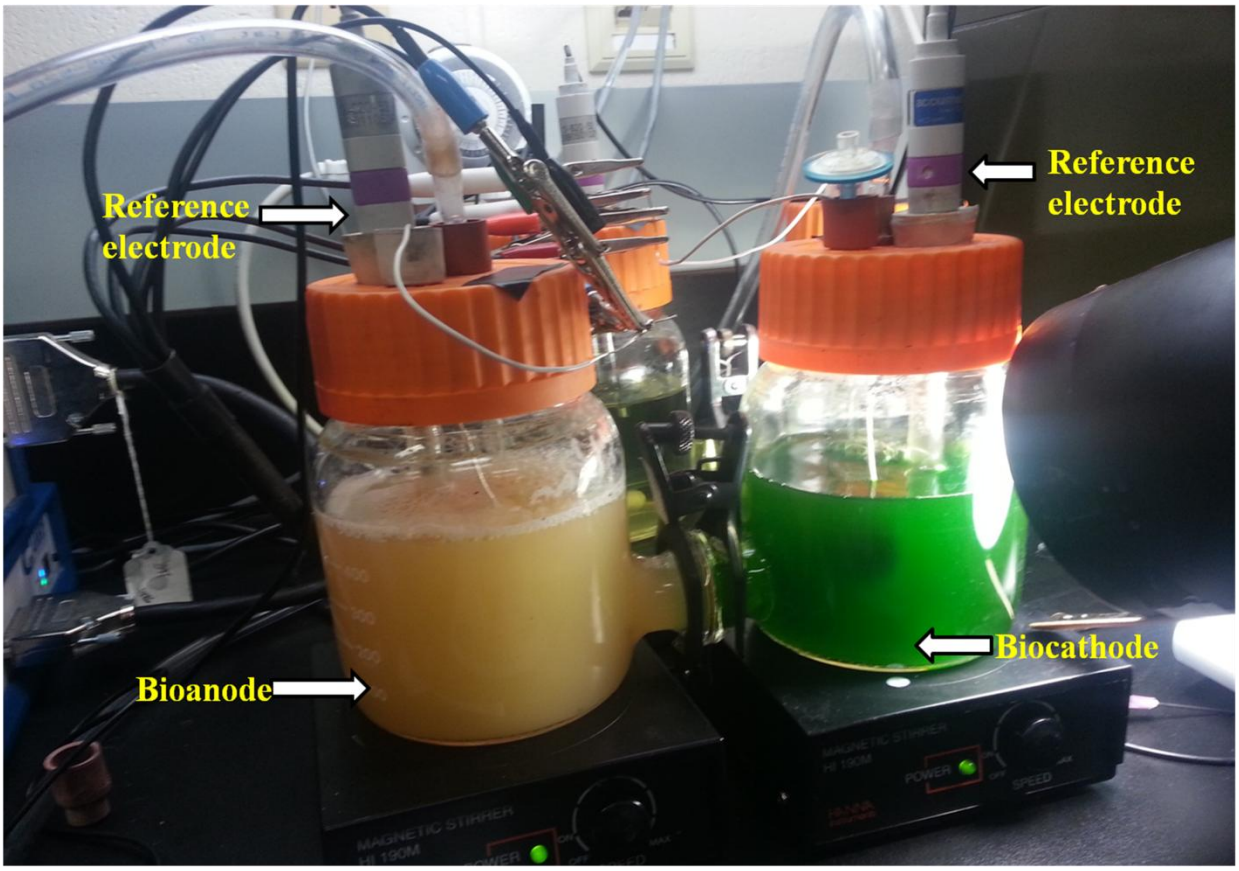

Figure 3.6 Complete bio-battery setup containing bacterial bioanode and photosynthetic algae biocathode. The bioanode contains composite electrode with immobilized bacteria (CNP-bacteria paste) and the biocathode contains composite electrode with CNP paste coating and *Chlorella vulgaris* suspended in the solution.

3.4 Analytical techniques and electrochemical tests

Analytical techniques such as Scanning Electron Microscopy (SEM) for analysis of electrode coatings, glucose concentration analysis of bioanodes and measurement of biomass concentration in the biocathode chamber by spectrophotometric analysis were done. The bioanode, biocathode and complete bio-battery setups were analyzed by measuring their open

circuit potentials and steady state polarization curves. Components of the internal resistance were determined through Electrochemical Impedance Spectroscopy (EIS) analysis.

3.4.1 NADH oxidation measurement of composite electrodes

The background currents from electrode materials should be measured without microbial species for obtaining meaningful results (Zhao *et al.*, 2009). After immobilizing the mediator, an oxidation test was performed with various concentrations of Nicotinamide Adenine Dinucleotide (NADH) to confirm bio-electrochemical activity, i.e., to determine whether the composite electrodes promote NADH oxidation. Cyclic voltammograms with a scan rate of 20 mV/s were performed between +0.4 V_{SCE} and -0.6 V_{SCE}.

3.4.2 SEM analysis of bioanode electrode coatings

Different configurations of electrodes were constructed for analysis; some composite electrodes were covered with CNP paste only, and some composite electrodes were covered with CNP-bacteria paste. For analysis, a small amount of the paste was taken from the electrode configurations and freeze dried until all the moisture is removed. Subsequently, the sample was placed on a sample holder and sputter coated with a conductive material (Gold nanoparticles) using EDWARDS S150B gold sputter coater to make them conductive and prevent charge build up on the sample. A Philips 505 Scanning Electron Microscope was used to analyze the samples.

3.4.3 Glucose concentration analysis of bioanodes

Concentration of glucose (substrate) in the anode chamber was analyzed to ascertain microbial growth and biochemical activity. Samples were drawn at different intervals from the anode chamber using a syringe fitted with a filter and analyzed in YSI^{tm} 2700 biochemistry analyzer.

3.4.4 Spectrophotometric analysis of algae biomass concentration

Biomass concentrations of the algae cultures were determined by measuring the optical densities using a spectrophotometer (Shimadzu Corporation, Kyoto, Japan) at a wavelength of 620 nm. Samples were taken from the biocathode chamber before and after experiments to compare the growth rates of the two algae species (*Chlorella vulgaris* and *Scenedesmus sp.*). Optical densities were converted to dry weight (mg/L) of microalgae using previously determined calibration curves.

3.4.5 Open circuit voltages

Open circuit voltages/cell potentials were measured with a potentiostat using the open circuit voltage experiment. For the bioanodes and complete bio-battery setup, the working leads were connected to the anode electrode while the counter and reference leads were connected to the cathode electrode. For the biocathode experiments, the working leads were connected to the cathode electrode while the counter and reference leads were connected to the anode and reference electrodes, respectively. The experiments were run for at least 48 hours and the final stable reading was taken as the cell potential.

3.4.6 Measuring and plotting polarization curves

Polarization curves can be used to determine the performance and the internal resistance of a MFC (Kim, 2011). Polarization plots with a slow potential sweep of 0.15 mV/s were conducted. This slow potential sweep allowed the scan to reach steady state at each point and provided a good representation of the voltage-current behavior. The current values from the potential sweep were divided by the 2-D projected surface area of the electrode to give the current densities and reported in mA/m^2. Subsequently, the power densities are determined and reported in mW/m^2.

3.4.7 Measuring internal resistances using EIS

In order to determine the resistances in each bio-battery, potentiostatic EIS experiments at the steady state open circuit voltage with an amplitude of 10 mV and a frequency range of 100 kHz to 0.1 Hz were conducted. Reference electrodes were placed in both the chambers. Data from the Nyquist plots were analyzed using Gamry^{tm} Echem Analyst software to determine the values of the bio-battery's ohmic resistance, charge transfer resistance, and diffusion resistance. To accomplish this, the data was fit to equivalent circuit models as discussed later in section 4.4.5. For the bioanode-chemical cathode setup, the impedance spectra were recorded using a two electrode mode (anode as working and cathode as counter and reference). For complete bio-battery setups, bioanode and biocathode impedance spectra were recorded individually using a three cell arrangement with the reference electrodes placed in their respective chambers, while the complete bio-battery's impedance spectra were recorded using a two electrode mode (cathode as reference) between the anode and the cathode. The membrane's contribution to ohmic resistance was determined by testing the anode with respect to the reference electrode placed in the cathode chamber or vice versa and subtracting it with the ohmic resistance contributed by the anode or cathode alone.

3.4.8 Measuring experimental uncertainty

The experimental uncertainty was determined by repeating the polarization curve and EIS measurements on separate experimental trials. For bioanodes, the average of three measurements was taken and plotted with standard deviation error bars. The uncertainty was also determined by looking at the open circuit variation of the biocathodes and complete bio-battery setups. For biocathode experiments, four separate experimental trials for composite electrodes with CNP coating and plain composite electrodes were conducted with two different species of algae

(*Chlorella vulgaris* and *Scenedesmus sp.*). For complete bio-battery experiments three separate trials were done.

4. RESULTS AND DISCUSSION

4.1 Development of composite electrodes

Type 304 stainless steel mesh based composite electrodes were prepared by two steps- 1) Electropolymerization of pyrrole on stainless steel mesh base and 2) Electropolymerization of methylene blue on polypyrrole coated stainless steel mesh. Polypyrrole is a conductive layer which prevents oxidation of metal and provides a base for redox mediator polymerization. Without the polypyrrole coating, the metal would preferentially oxidize at potentials required for mediator polymerization. Polypyrrole is conductive when subjected to potentials between -0.5 V_{SCE} and 1.2 V_{SCE}. This is primarily because, below -0.5 V_{SCE}, the doping ions (salicylate) leave the solution rendering the film insulating, while above 1.2 $V_{SCE,}$ over oxidation occurs and degrades the film (Godwin, 2011). Salicylate was found to be a stable doping anion which prevents metal dissolution from occurring (Godwin, 2011).

Figure 4.1 shows the chronopotentiometry plot for the electropolymerization of pyrrole on a stainless steel mesh. The initial low potential region indicates metal dissolution in the solution, followed by a sudden increase in the potential denoting the formation of metal-salicylate layer which prevents further metal dissolution from occurring, and the gradual subsequent decrease in the potential indicates the formation of polypyrrole layer on the electrode surface.

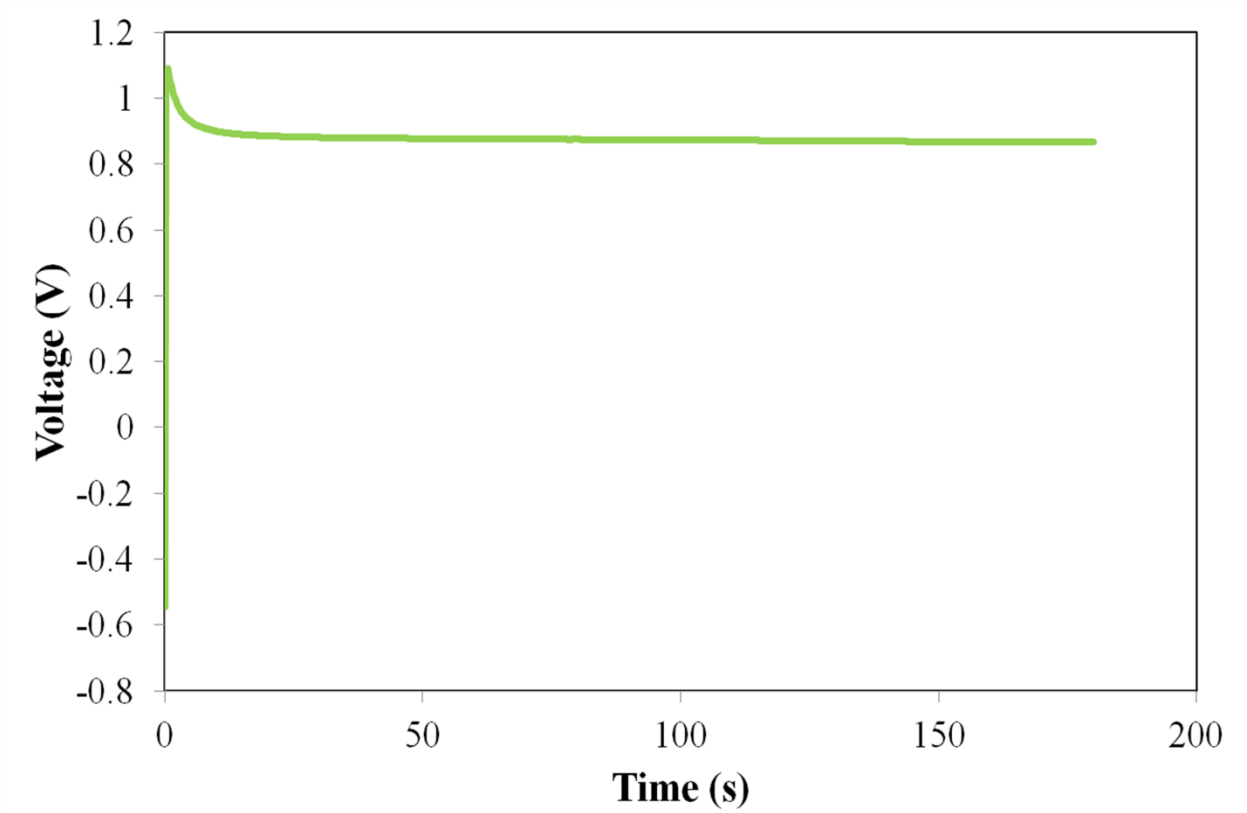

Figure 4.1 Chronopotentiometry plot for polypyrrole formation on 304L stainless steel mesh. The solution required for polypyrrole formation contained 0.350 mol/L pyrrole, 0.080 mol/L salicylate.

Polymerization of the redox mediator (Methylene blue) was achieved by cyclic voltammetry sweeps. Attempts were made in literature to polymerize methylene blue directly on non-noble substrates like stainless steel and it was noticed that the metal started to oxidise rapidly at potentials of 1 V and prevented the formation of methylene blue (Godwin, 2011). 8 to 12 cyclic voltammetry sweeps between -0.4 V_{SCE} and 1.05 V_{SCE} provided a uniform layer of methylene blue which could be visually seen as a purple coating on the metal as shown in Figure 4.2. It was also observed in literature that if the lower switching potential went below -0.5 V, the polymerization was non uniform as the polypyrrole became non-conductive by losing its doping ions (Godwin, 2011).

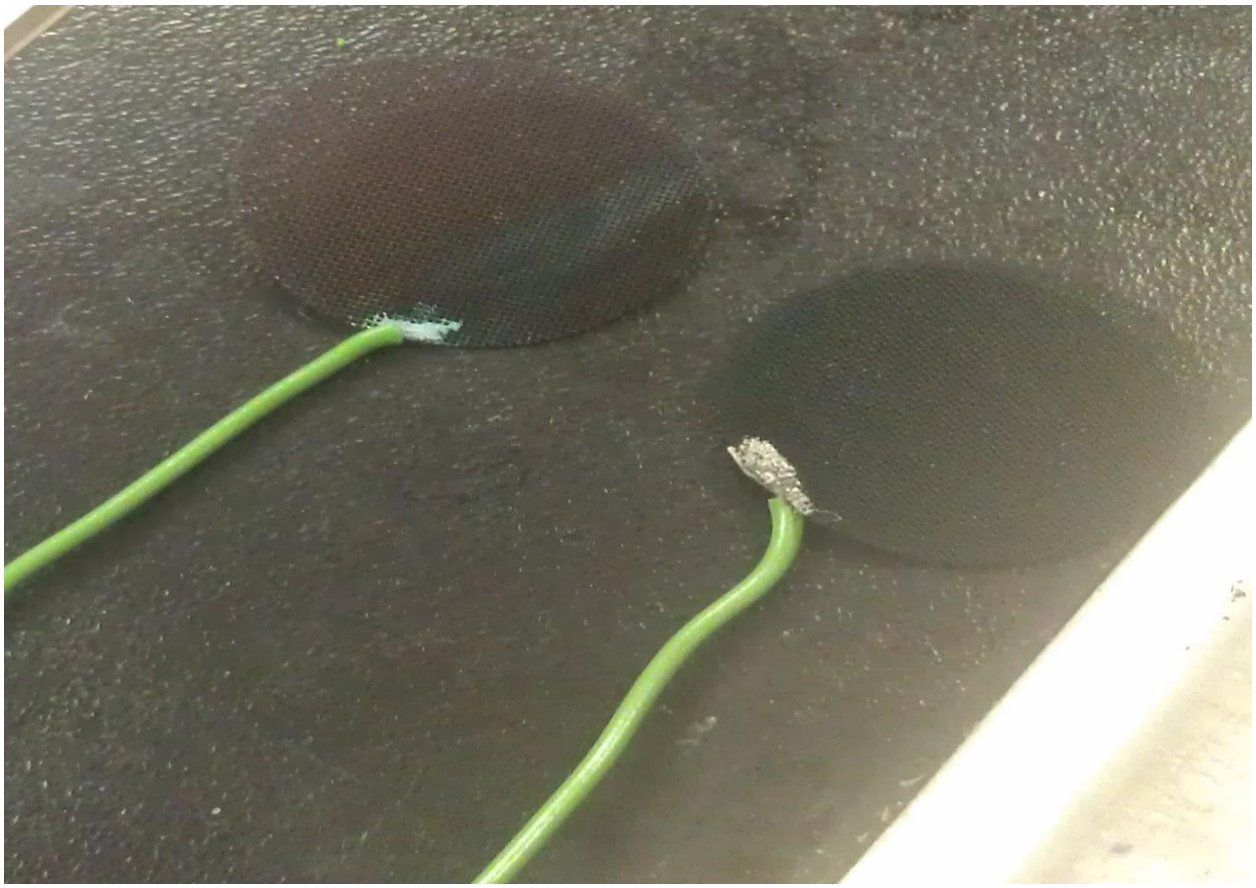

Figure 4.2 Pyrrole-Methylene blue coated (left) and Polypyrrole coated (right) electrodes.

4.2 NADH oxidation measurement

The composite electrodes were tested for bioelectrochemical activity readiness by immersing them in solutions containing different concentrations of NADH. Cyclic voltammetry sweeps between +0.4 V_{SCE} and -0.6 V_{SCE} at a scan rate of 20 mV/s were run to determine the oxidation peaks (maximum current on the cyclic voltammetry curve) for different concentrations of NADH. NADH oxidations on the composite electrodes were confirmed by the increasing oxidation peak with the increase in NADH concentration (Figure 4.3).

The plot of oxidation peak versus NADH concentration is linear indicating the biochemical activity happening on the electrode surface. Moreover, there was some background current (262 µA) present even when there was no NADH present in the solution. This background current is

useful for microbial fuel cell operations where high steady state currents are required (Godwin, 2011).

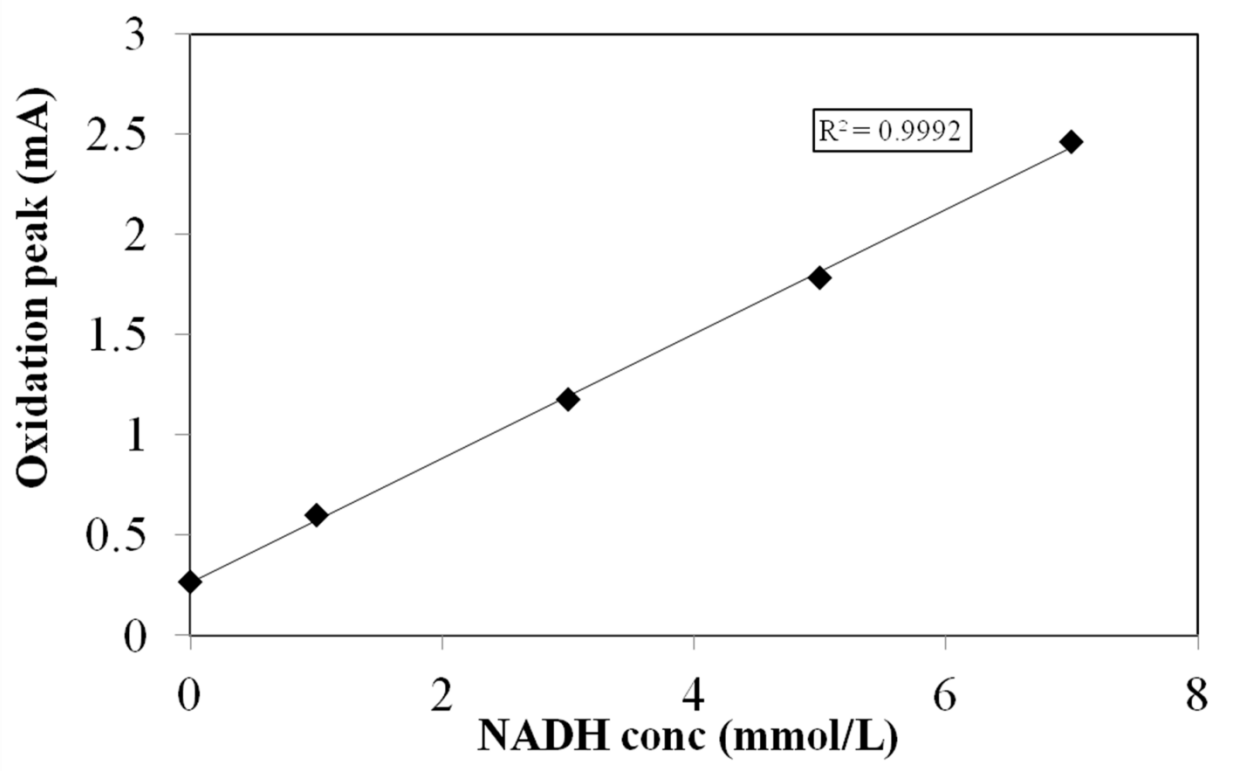

Figure 4.3 NADH oxidation plot on composite mesh electrode at varying concentrations of NADH. Each datum point represents the oxidation peaks of cyclic voltammetry scans for varying concentration of NADH at a scan rate of 20 mV/s.

4.3 SEM image of bacteria-carbon paste coating

Scanning electron microscopy is used by researchers to characterize the electrode coatings and bio-films on the electrodes. Figure 4.4 shows SEM images of these electrodes covered with CNP paste, (a) without, and (b) with, *Escherichia coli* K-12 bacteria. Each bacterium, which is rod shaped and white in the figure, can be clearly seen attached to the carbon particles in the lower right-hand portion of Figure 4.4b. Figure 4.4a does not show any white rod shaped bacterium.

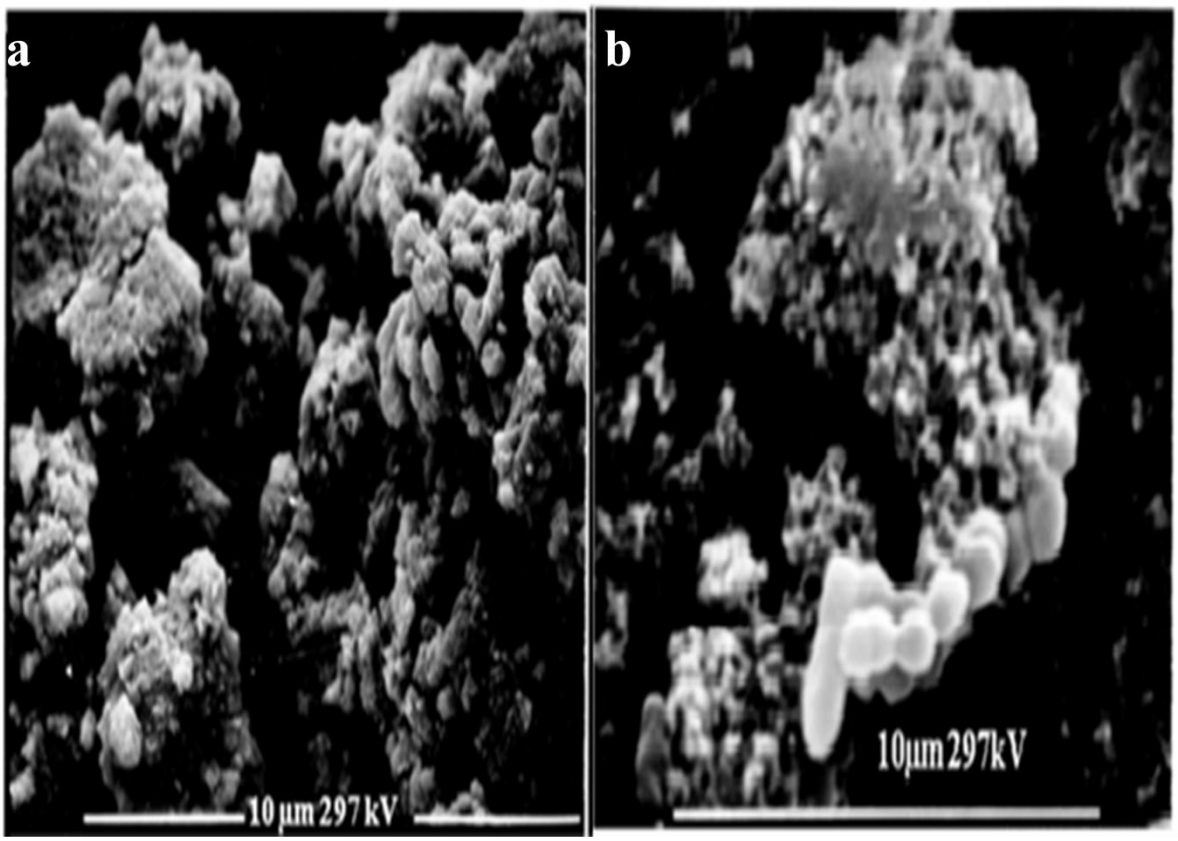

Figure 4.4 SEM images of composite electrodes (a) with only carbon paste and (b) with carbon paste and bacteria.

4.4 Bioanodes with composite electrodes and CNP-bacteria paste

The first phase of the research involved testing of the composite electrodes with CNP-bacteria coating against chemical cathodes containing potassium ferricyanide. The primary methods used to evaluate the bio-battery performance were open circuit potential, polarization curves and electrochemical impedance spectroscopy analysis. Polarization curves were plotted by running potential sweeps at a slow scan rate (0.15 mV/s) between open circuit and short

circuit potentials. Electrochemical impedance spectroscopy analysis was conducted at steady state open circuit potentials to determine the internal resistance components in the fuel cell.

4.4.1 Representative cyclic voltammetry plots

Cyclic voltammetry sweeps at a scan rate of 0.15 mV/s were used to plot the current versus voltage. This slow sweep rate allowed the scan to reach steady state at each point and provided a good representation of the voltage-current behavior similar to that conducted by Hoffman *et al.* (2013). Figure 4.5 shows the cyclic voltammetry plots for the bioanode experiments incorporating a composite electrode with CNP-bacteria paste coating and composite electrode with bacteria suspended in the solution (control setup).

The composite electrode with CNP-bacteria coating produced a higher short circuit current than the composite electrode with bacteria suspended in the solution, as shown in figure 4.5. This could be due to the increased surface area and improved conductivity created by immobilizing the mediator and bacteria directly on the surface of the composite electrodes.

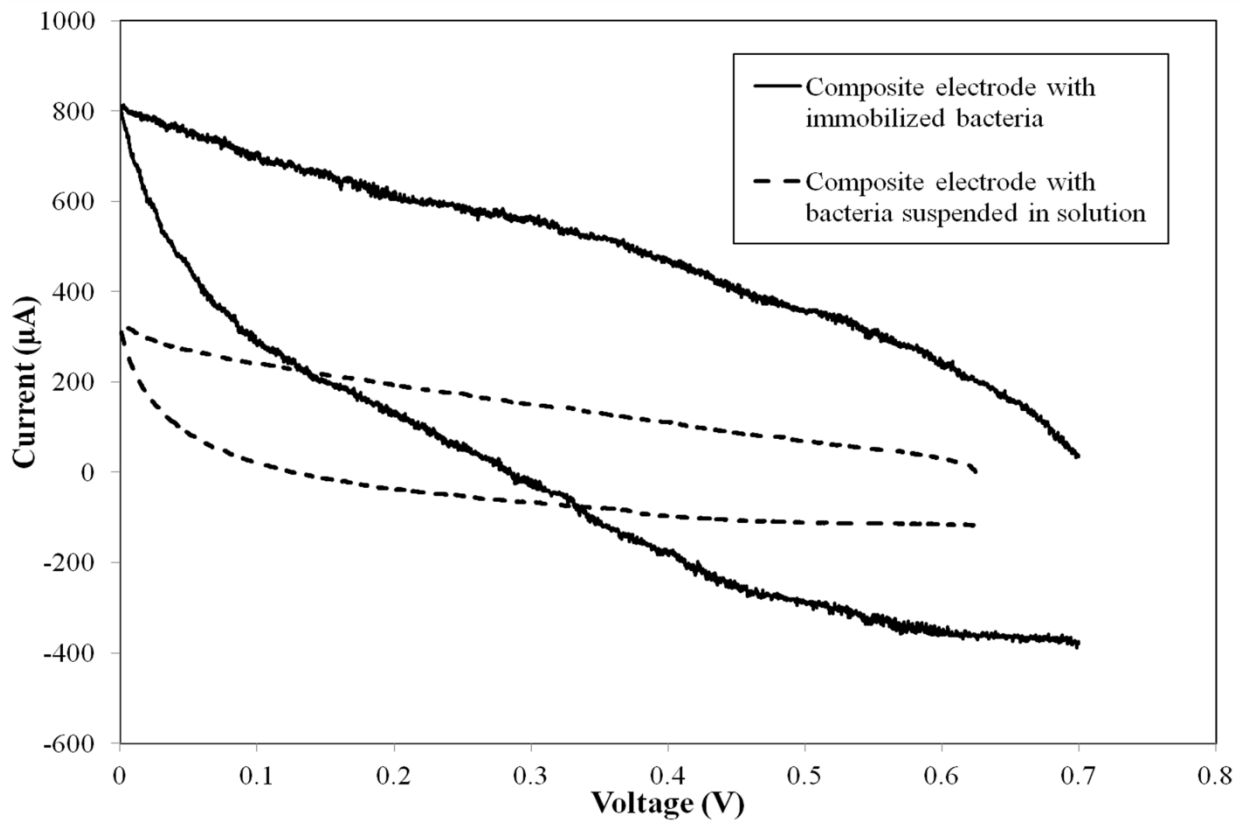

Figure 4.5 Representative cyclic voltammetry plots for bioanodes with immobilized and suspended bacteria. The composite electrode with CNP-bacteria coating produces higher short circuit current than plain composite electrodes with bacteria suspended in solution.

4.4.2 Performance assessment of bioanode fuel cells

The performance of bioanodes was assessed by polarization curves that plotted the voltage versus current density and power density curves. A power density curve displays the maximum power output from a system with its corresponding current density. The substrate concentration was also monitored to confirm the biochemical activity in the anode chamber. Figure 4.6 shows the polarization curve for a composite electrode with immobilized bacteria (CNP-bacteria paste) compared with the polarization curves for composite electrodes in other configurations. These alternate configurations include: Case I, a composite electrode with immobilized CNP paste and

bacteria suspended in solution, and Case II, a composite electrode with bacteria suspended in solution. The composite electrode with immobilized bacteria (CNP-bacteria paste) produced an average short circuit current density of 1506 mA/m^2, almost a 53% increase when compared with current densities of Case I and Case II. Moreover, Case I produced approximately 13% more current density than Case II. This could likely be due to carbon nanoparticles facilitating better electron transfer by increasing the conductivity and surface area for bacterial adhesion.

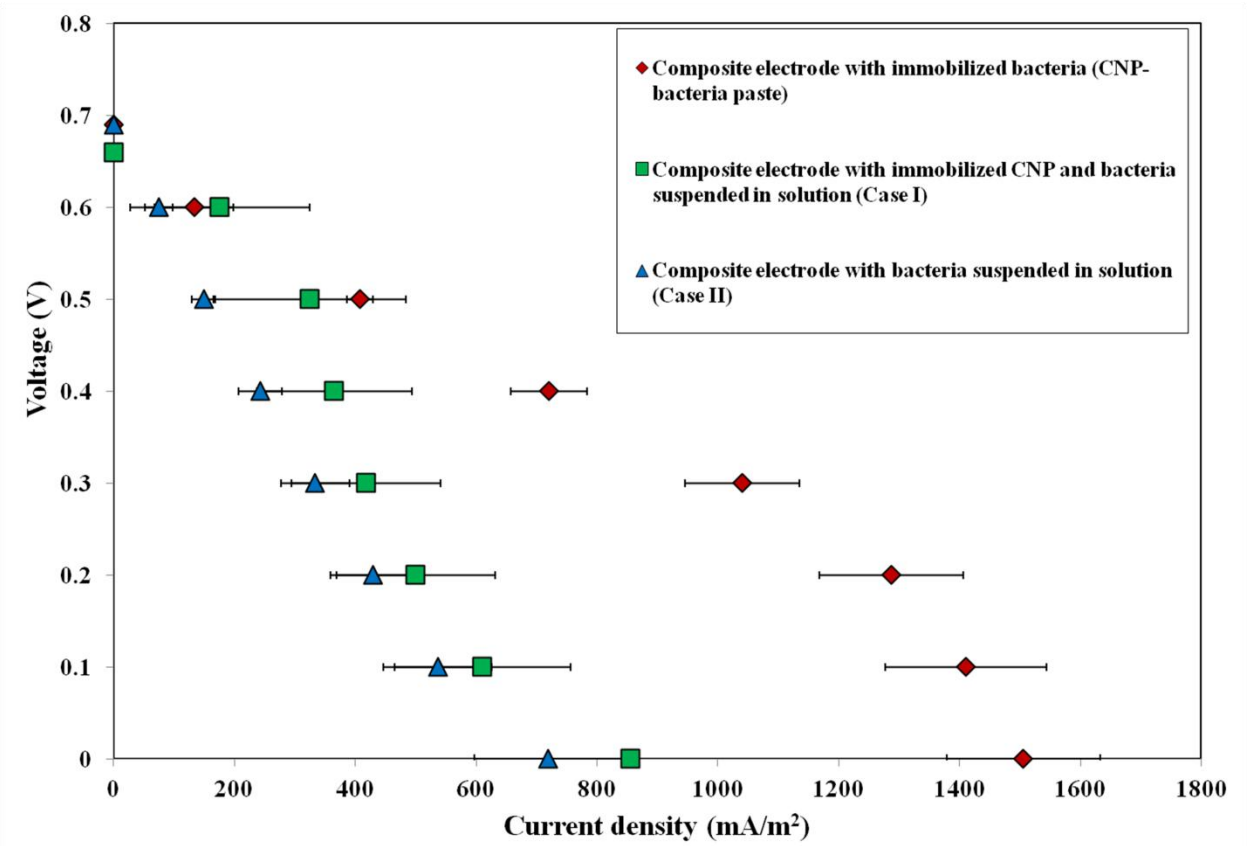

Figure 4.6 Polarization curves of composite electrode with immobilized bacteria compared with other composite electrode configurations. Error bars represent standard deviation of current measurement.

Figure 4.7 shows the power density curves of a composite electrode with immobilized bacteria (CNP-bacteria paste) and other electrode configurations. The composite electrode with

immobilized bacteria achieved an average power density of 331 mW/m^2. This is almost 69% more than the other configurations with suspended bacteria (Cases I and II).

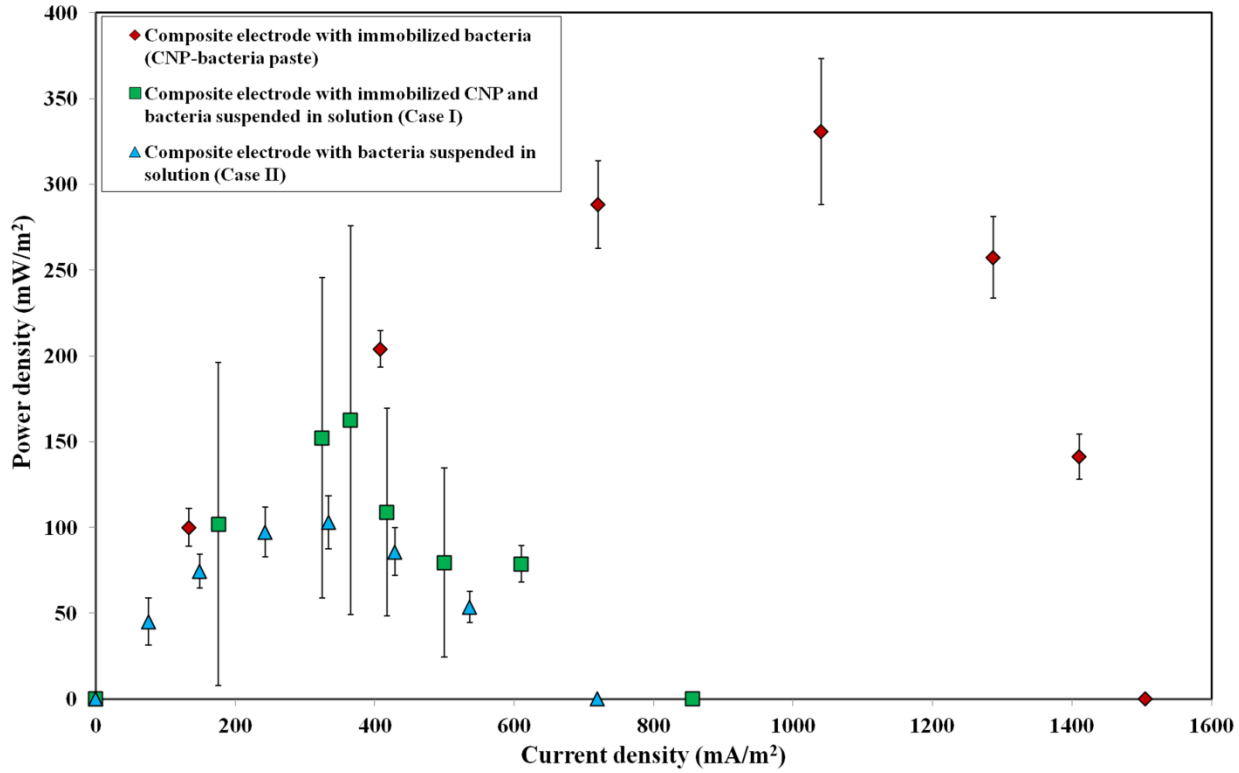

Figure 4.7 Power density curves of composite electrode with immobilized bacteria compared with other composite electrode configurations. Error bars represent standard deviation of power measurement.

4.4.3 Effect of Teflon^{tm} and CNP amounts on bioanode performance

The amount of Teflon^{tm} added to bind the carbon nanoparticles and bacteria greatly affects the performance of the bioanode. Higher amounts of Teflon^{tm} will insulate the electrode surface to charge transfer, while lower amounts will not sufficiently bind the bacteria and carbon nanoparticles (Yuan *et al.*, 2009). Figure 4.8 shows the change in power density with various amounts of Teflon^{tm} used in the CNP-bacteria paste applied to the composite anode. As seen in

figure, 0.5 mL and 1.5 mL of Teflon^{tm} produced lesser power than 1.0 mL of Teflon^{tm}. This data was also in accordance with previous research conducted by Yuan *et al.* (2009).

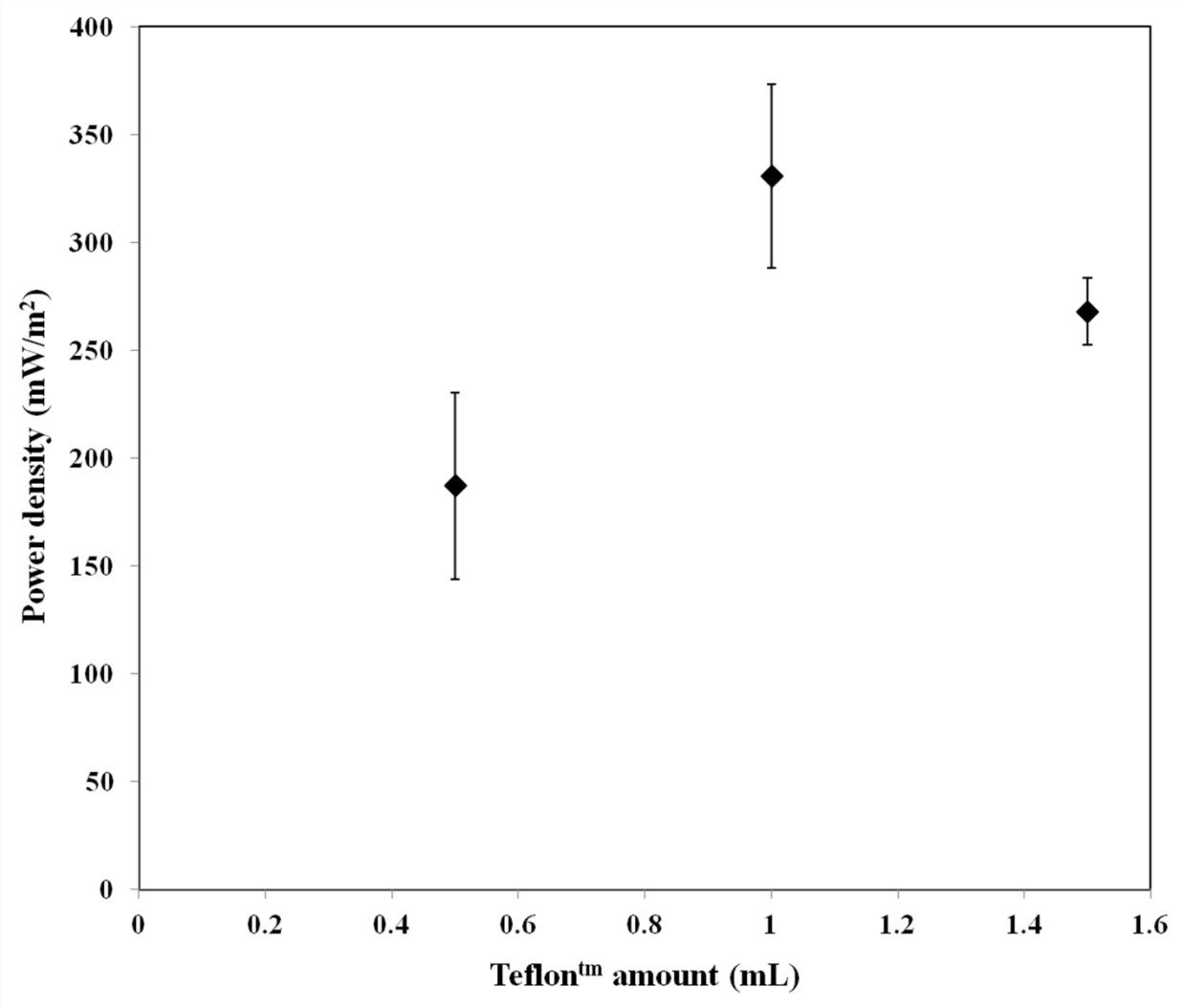

Figure 4.8 Effect of Teflon^{tm} amounts on power density. Error bars represent standard deviation of power measurement. 1mL of Teflon^{tm} produced higher power output than 0.5 and 1.5 mL.

The electrode performance was also studied by varying the amounts of Carbon Nanoparticles (CNP). Three different amounts of Vulcan XC-72R, 0.2. 0.3 and 0.4 g were used to create the

CNP-bacteria paste applied to the surface of the composite electrode. Figure 4.9 shows the average power density plots for various CNP amounts.

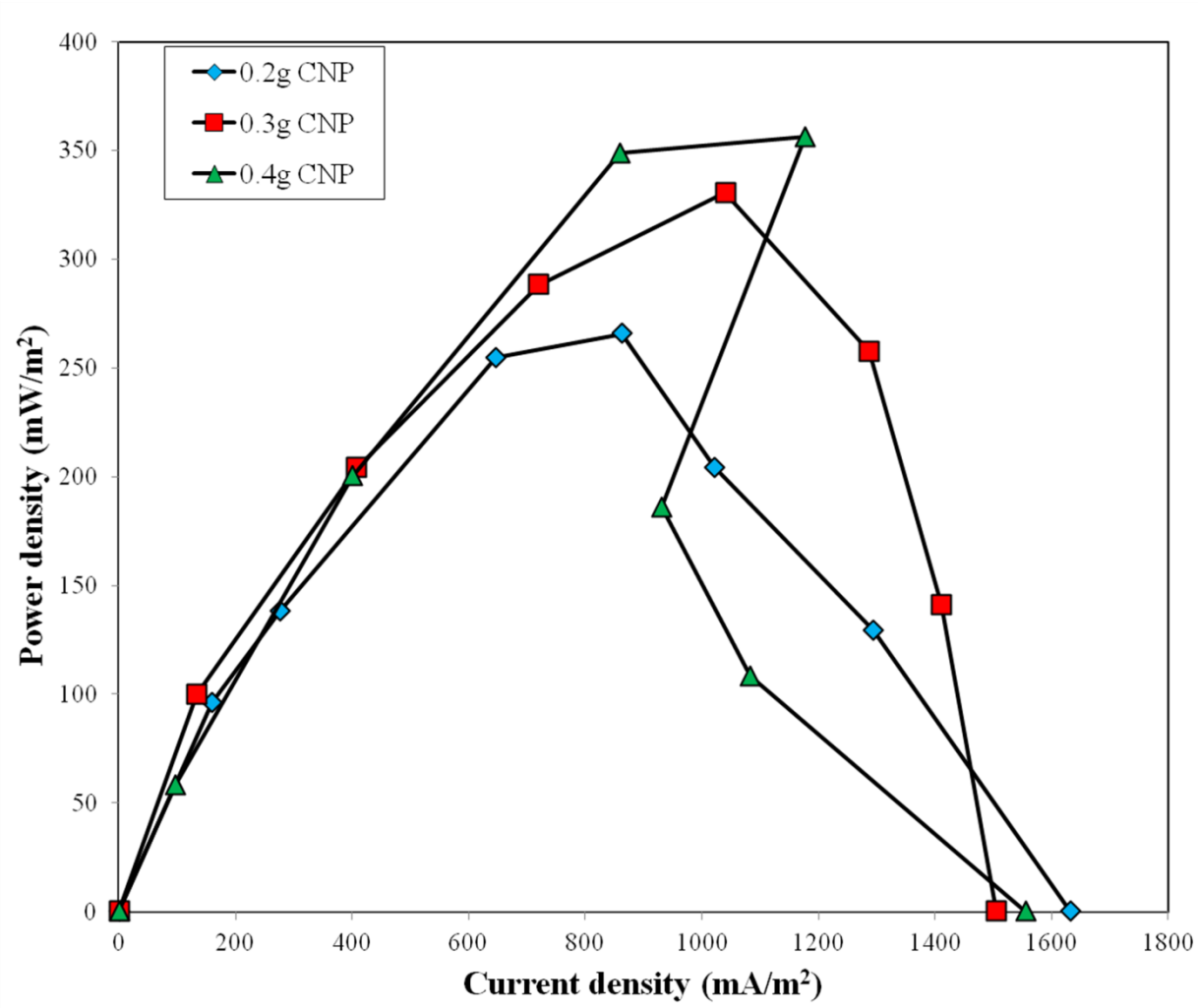

Figure 4.9 Effect of carbon nanoparticle amounts on fuel cell performance. 0.2, 0.3 and 0.4 g of CNP produced almost the same current output with slight variations in power output. Lines are used to help the reader follow the data points.

As seen from the figure, the maximum power density using 0.2 g of CNP was slightly lower than maximum power densities using 0.3 and 0.4 g of CNP, but not significantly so. It is also to be noted that the current densities were almost the same for these amounts. This supports the fact

that the inner part of CNP made little or no impact on power production and only the CNP and bacteria on the surface or closer to the surface acted as catalyst and produced power (Yuan *et al.*, 2009). For bioanode experiments using *E. coli K-12* and composite mesh electrodes, 0.3 g of CNP with 1 mL Teflon^{tm} for 0.001 mol/L methylene blue was found to be the optimum amount which gave reproducible results (based on standard deviation error bars of three separate experimental setups).

4.4.4 Concentration of glucose in the bioanode chamber

The concentration of substrate (glucose) in the anode chamber was analyzed to ascertain microbial growth and biochemical activity. Figure 4.10 shows the change in glucose concentration with time. The glucose concentration decreases with time and this could likely be due to the biochemical activity (bacteria metabolization) in the anodic chamber.

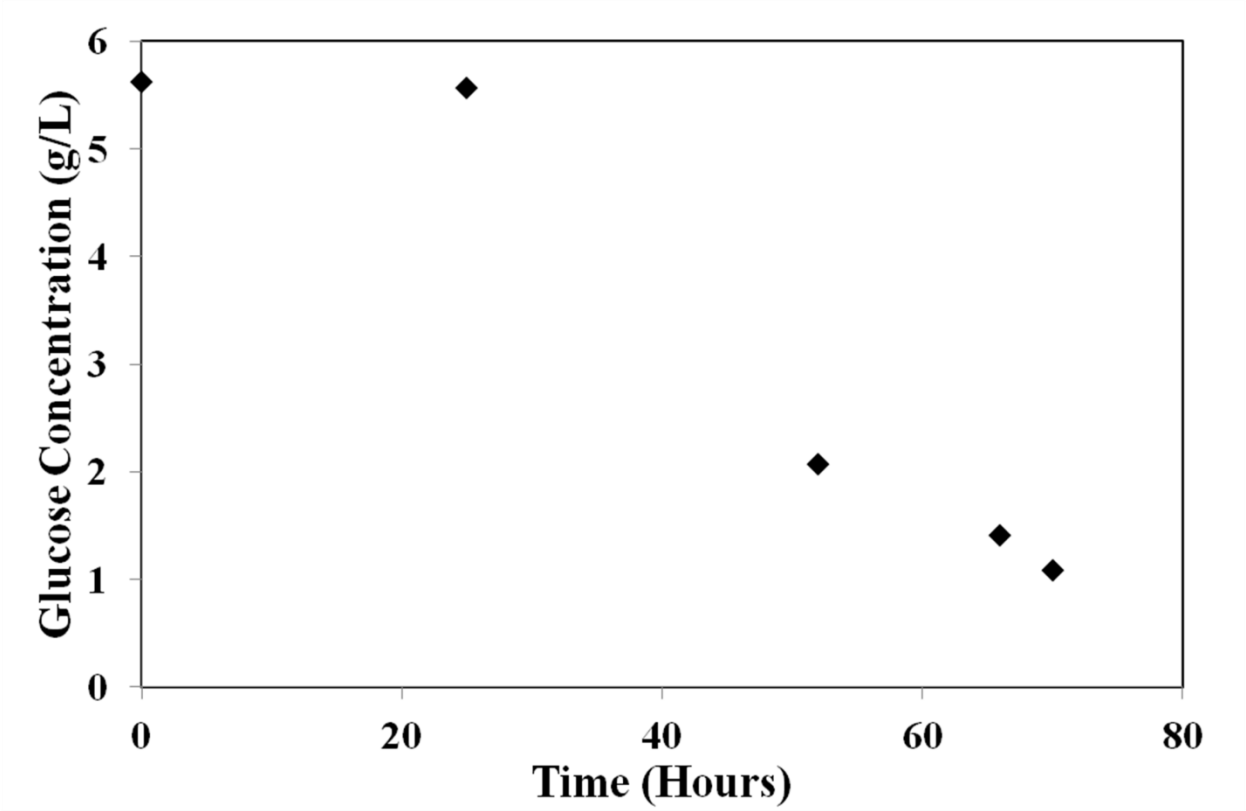

Figure 4.10 Glucose concentrations in the anode chamber. The glucose concentration decreases with time as the bacteria metabolizes.

4.4.5 EIS analysis of bioanodes

The overall internal resistance in a bioanode is comprised of ohmic resistance, charge transfer resistance and diffusion resistance. Ohmic resistance constitutes the resistances of ion conduction through the anode solution, cathode solution and the cation exchange membrane. Charge transfer resistance constitutes the resistance of the transfer of charge between the solid conductor (electrodes) and solution. In this case, for the bioanode, this includes the resistance within microbial metabolism, transfer of charge from the microbe to the mediator, and transfer from the mediator to the anode. Diffusion resistance constitutes the resistance caused by a build-up of concentration gradients within the bioanode. In order to determine these individual

resistances, potentiostatic EIS experiments at steady state cell potential (Open circuit) with an amplitude of 10 mV and frequency range of 100 kHz to 0.1 Hz were conducted in a two electrode mode (cathode as reference). Figure 4.11 shows the nyquist plots obtained for two different bioanode electrode configurations. The first bioanode incorporated a composite electrode with immobilized bacteria (CNP-bacteria paste) and the second bioanode incorporated a composite electrode with bacteria suspended in the solution. In the nyquist plots, the initial value on the real impedance axis represents the Ohmic resistance, and the diameter of the semicircle formed by the data immediately above the real axis, corresponds to the charge transfer resistance. As seen in Figure 4.11, the magnitude of the impedance spectra for the composite electrode with immobilized bacteria (CNP-bacteria paste) setup was smaller than the setup with a composite electrode and bacteria suspended in the solution.

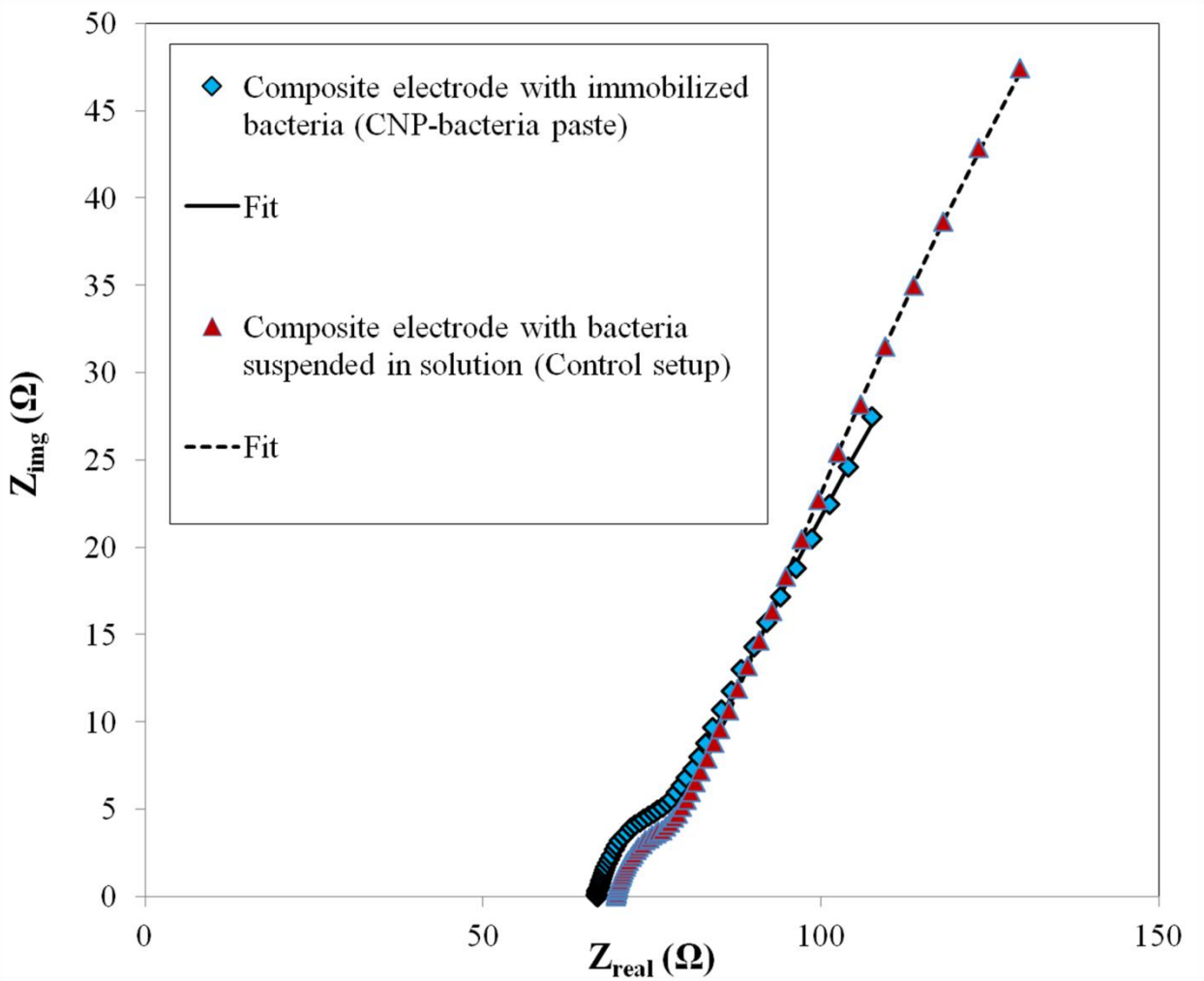

Figure 4.11 Nyquist plots for bioanodes incorporating a composite anode with immobilized bacteria and composite anode with bacteria suspended in solution. Data points are fit using equivalent circuit models.

Data from these Nyquist plots were analyzed using Gamry^{tm} Echem Analyst software to determine the values of the bioanode internal resistances (Ohmic resistance, charge transfer resistance, and diffusion resistance). To accomplish this, the data was fit to two models. Figure 4.12 shows the two equivalent circuit models. Model 1 is a Randles circuit used to determine the overall charge transfer resistance, Ohmic resistance, and diffusion resistance, of the entire fuel

cell. In this model, R_u is the Ohmic resistance, R_{ct} is the charge transfer resistance with cpe as its corresponding constant phase element (with parameter 'a' ranging between 0 and 1 representing a resistor and an ideal capacitor respectively), and Z_W is the Warburg impedance for diffusion with R_L as its associated resistance. Model 2 is commonly employed for dual chambered MFCs (He and Mansfeld, 2009) and is used to determine the charge transfer contributions of anode and cathode separately along with the Ohmic resistance. R_c and R_a represent the individual charge transfer resistances of the cathode and anode respectively with Y_{oc} and Y_o their associated constant phase elements.

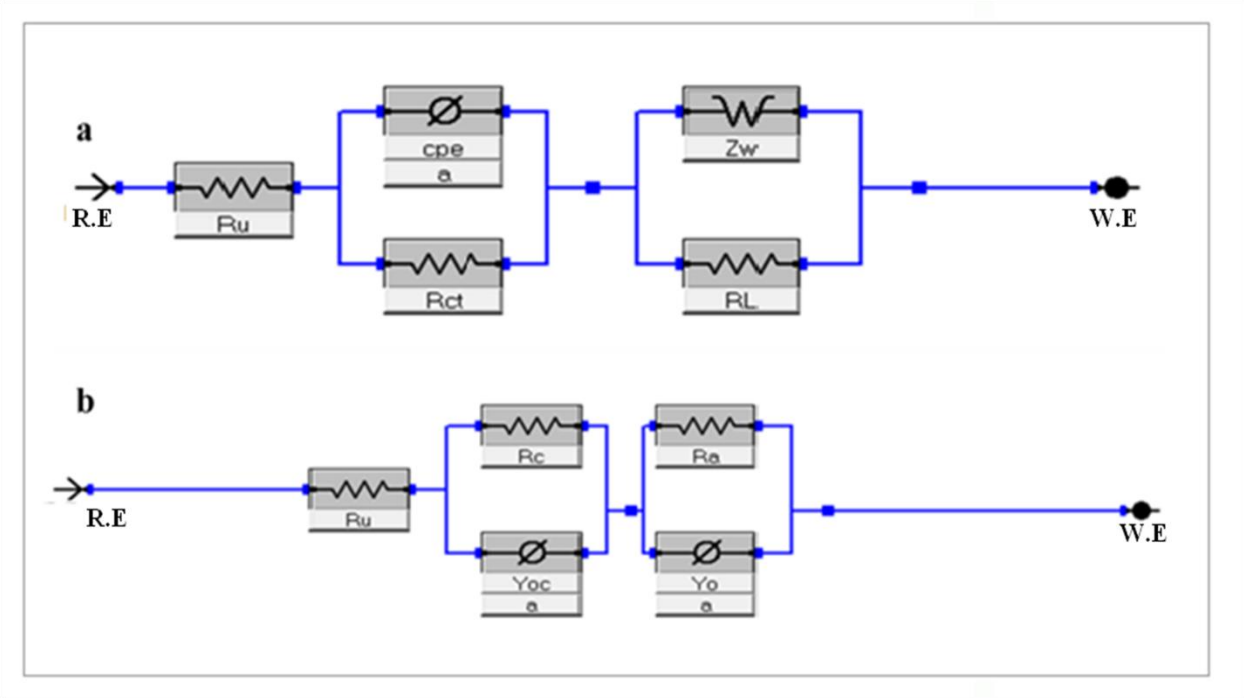

Figure 4.12 Model 1 (a) and Model 2 (b) for EIS data fit. Model 1 is used for determining the overall charge transfer resistance of the fuel cell setups while Model 2 is used for determining the individual charge transfer resistance contributions of the anode and cathode.

Figure 4.13 shows a comparison of the internal resistances in bioanodes with two different configurations. The first bioanode incorporated a composite electrode with immobilized bacteria (CNP-bacteria paste) and the second bioanode incorporated a composite electrode with bacteria suspended in solution. As seen from the figure, charge transfer resistance was significantly larger than both Ohmic resistance and diffusion resistance, with approximately 80% of the overall internal resistance, for both configurations. Figure 4.13 also shows that the composite electrode with immobilized bacteria had a reduction in the overall charge transfer resistance by approximately 51%. Additionally, there was no significant difference in Ohmic and diffusion resistances between the two configurations. In fact, the diffusion resistance appears to be negligible in both configurations, which is in accordance with previous research conducted using stainless steel electrodes with immobilized mediator (Godwin, 2011).

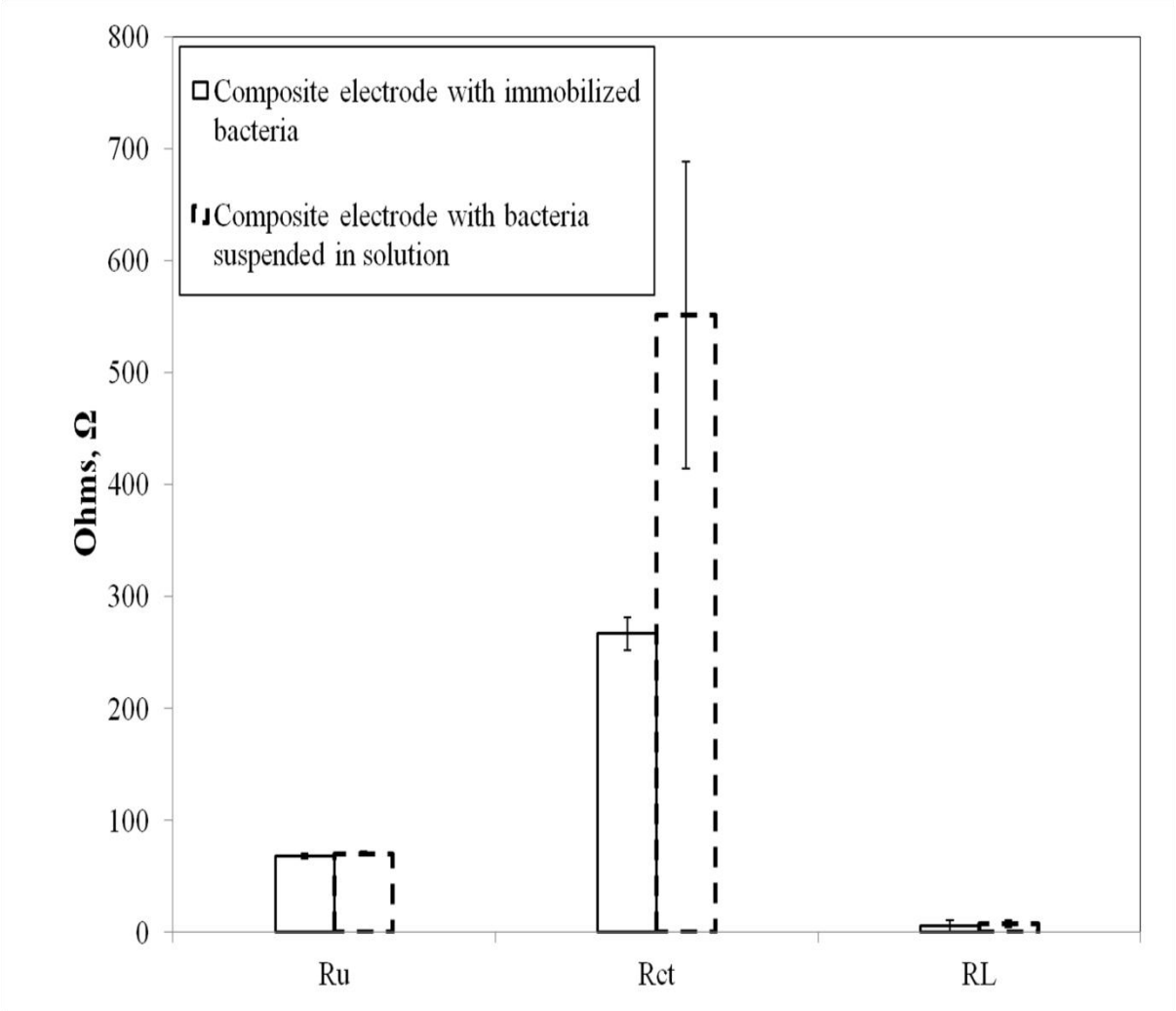

Figure 4.13 Internal resistances comparison of composite electrode with immobilized bacteria and composite electrode with bacteria suspended in solution. Charge transfer resistance is the dominant one in bioanodes with diffusion resistance being almost negligible. Error bars represent standard deviation of impedance measurement.

Through the application of model 2 in Figure 4.12, it was determined that the charge transfer resistance at the anode (R_a) was higher than the charge transfer resistance at the cathode , as shown in Table 4.1. This behavior could be attributed to the kinetically sluggish oxidation process at the anode compared to the reduction of ferricyanide at the cathode, as previously

determined (Ramasamy *et al.*, 2008). Moreover, the R_c for both the configurations were quite similar with 11.95 Ω and 9.092 Ω for the composite electrode with immobilized bacteria (CNP-bacteria coating) and composite electrode with bacteria suspended in the solution setups, respectively. This is due to the same catholyte (ferricyanide) used for both the setups. The constant phase element of the anode (Y_o) was also higher than the constant phase element of the cathode (Y_{oc}), which could be attributed to the increased surface area of the anode by the carbon nanoparticles (Hosseini and Ahadzadeh, 2012). The proton exchange membrane's (PEM) contribution can be determined by measuring the ohmic resistance of bioanode chamber alone and subtracting it with the ohmic resistance contributed by bioanode chamber and membrane together (determined by placing the reference electrode in the cathode chamber). The PEM contributed to approximately 95% of the ohmic resistance with the anode and anolyte (anodic chamber) contributing 3.6 Ω and membrane contributing 62 Ω in this type of fuel cell.

A check was conducted to confirm the values of internal resistance provided by the Gamry^{tm} Echem Analyst software. From Figure 4.6, from the slope of the polarization curves, the average overall internal resistance for each bioanode can be calculated. From these slopes it can be clearly seen that the overall internal resistance of the MFC incorporating a composite anode with bacteria suspended in solution is approximately double that of the MFC incorporating a composite anode with immobilized bacteria. These findings, from Figure 4.6, support the findings from the EIS analysis. These results demonstrate the improved charge transfer and increased surface area due to immobilization of the bacteria upon the composite electrode.

Table 4.1 Electrochemical Impedance parameter comparison of the two anode configurations.

Configuration	**R_u (Ω)**	**R_a (Ω)**	**R_c (Ω)**	**Y_o ($S*s^a$)**	**Y_{oc} ($S*s^a$)**	**a**
Composite electrode with immobilized bacteria	66.53±1.7	**169±5**	**12.0±2.3**	0.03±0.01	0.005±0.001	0.580
Composite electrode with bacteria suspended in solution (Control setup)	69.32±1.05	**550±91**	**9.1±3.1**	0.017±0.005	0.003±0.002	0.546

4.4.6 Literature comparison to other E. coli K-12 based MFC studies.

Modifications to anodes incorporated into MFC have been studied by researchers and significant improvements in power densities following the addition of Carbon Nano Tubes (CNT) and Carbon nanoparticles (CNP) have been noted. However, due to the variations in electrode surface areas and difference in metabolism of different microorganisms, it can be difficult to directly compare the performance of MFCs. The current study, focusing on composite electrodes with immobilized bacteria, achieved 1645 mA/m^2 of current density and a power density of 378 mW/m^2. The research here was done using bio-batteries; however, the results are applicable to MFCs and can be compared. Table 4.2 shows a comparison of current study with other *E. coli K-12* MFC studies. From Table 4.2, it can be seen that the composite electrode with CNP-bacteria paste displays improved current and power densities when compared with other values from the literature.

Table 4.2 Comparison of current study with literature. Comparison was done with other studies that used E. coli K-12 as anode catalyst and electrode modifications

Comparison Parameter	**Current study**	**Ming *et al.*, 2008.**	**Qiao *et al.*, 2007.**	**Park *et al.*, 2003.**	**Park *et al.*, 2000.**	**Davilla *et al.*, 2008.**	**Hoffman *et al.*, 2013.**
Max current density, mA/m^2	**1600±100**	612.50	~145	325	31	-	316
Max power density, mW/m^2	**380±20**	166.67	42	91	-	7.89	39.35

4.5 Photosynthetic Biocathodes with composite electrode and CNP coating

Biocathodes were operated using 20 mM ferrocyanide as the electron donor in the anode. Tests were conducted with respect to the reference electrode placed in the anode chamber due to the unstable nature of ferrocyanide and to give consistent results. Two different composite electrode configurations were tested: 1) Composite electrode with CNP coating and 2) composite electrode without CNP coating. Two different species of algae (*Chlorella vulgaris* and *Scenedesmus sp.*) were also tested.

4.5.1 Biocathode open circuit potentials

The open circuit potentials were measured between the composite electrodes with CNP coating in the biocathode and reference electrodes in the ferrocyanide anode using the Gamry

Reference 600 potentiostat. When the biocathode was inoculated with the starter culture of algae, the solution was pale green in color. But as growth continued in the biocathode chamber, the solution turned dark green and bio-film could be seen forming on the electrode.

It was noticed that the open circuit potentials were higher once the algae bio-films formed on the electrode surface. This increase in potential is due to the enhanced growth rate and interaction of the microbes with the electrode surface (Godwin, 2011). Figure 4.14 shows the open circuit potentials (OCP) of the biocathodes containing *Chlorella vulgaris*, *Scenedesmus sp.* and control setup without algae. In the control setup without algae, mixture of air and CO_2 was passed into the cathode chamber and as shown in the figure, the OCP was lower than biocathode setups containing algae. Moreover, the control setup was started with only CO_2 and a drop in potential could be seen on the open circuit potential plot. But, as soon as air was introduced, the potential started to rise. This could be because of air facilitating the reduction process at the cathode.

The reproducibility of steady state open circuit potential was acceptable with voltages ranging between 0.20 and 0.14 V, based on 3 separate experimental trials with supplemental CO_2 and composite electrodes with CNP coating. The likely cause of experimental variation is due to the bio-fouling of membrane and different growth yields of algae. Also, the composite electrodes with CNP coating showed some variability due to slight differences in steel surface, ageing of polypyrrole, CNP coating thickness and general electrode placement.

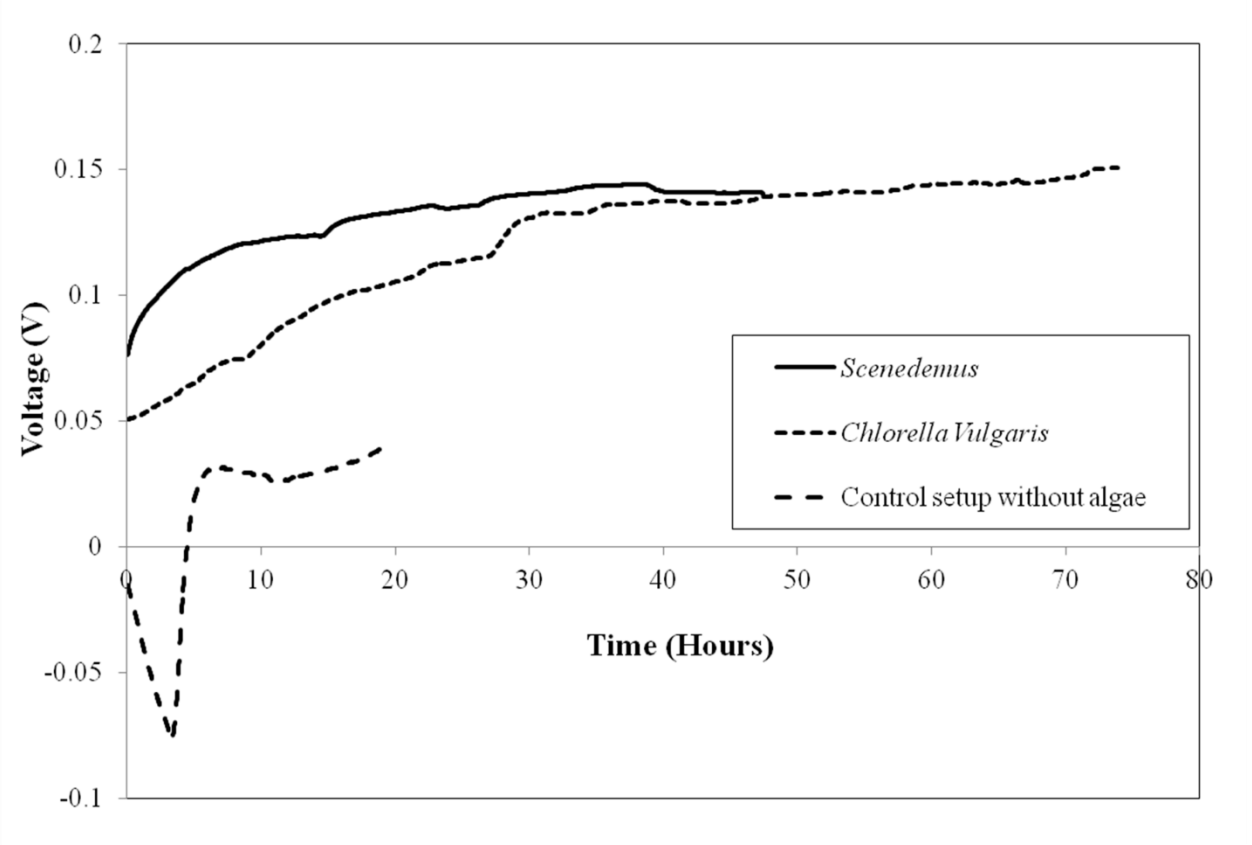

Figure 4.14 Open circuit potentials of biocathode setups with *Chlorella vulgaris* and *Scenedesmus sp.* compared with the control setup without algae.

4.5.2 Polarization curve comparison of biocathodes

The polarization curves of biocathodes with two different electrode configurations (composite electrode with CNP coating and composite electrode without CNP coating) and two different species of algae (*Chlorella vulgaris and Scenedesmus sp.*) are shown in Figure 4.15. Current density was calculated by dividing the current values by the 2-D projected surface area of the electrode (5.1 cm^2). The composite electrodes with CNP coating produced higher current density than composite electrodes without CNP, approximately 27% more than plain composite electrode biocathode setups. Even though performance of biocathodes containing *Chlorella vulgaris* and *Scendemus sp.,* using composite electrodes with CNP coating were somewhat

similar, with average current densities of 225 mA/m^2 and 250 mA/m^2, the growth rates were considerably lower in the case of the latter (450 mg/L Vs 2250 mg/L, determined through spectrophotometric analysis). The standard deviations of current measurements were also significantly larger. The biocathodes based on *Chlorella vulgaris* gave more reproducible results (smaller standard deviation) and were used for complete bio-battery experiments. The control setup had only carbon dioxide and air passed into the cathode chamber and did not have any algae suspended in the solution.

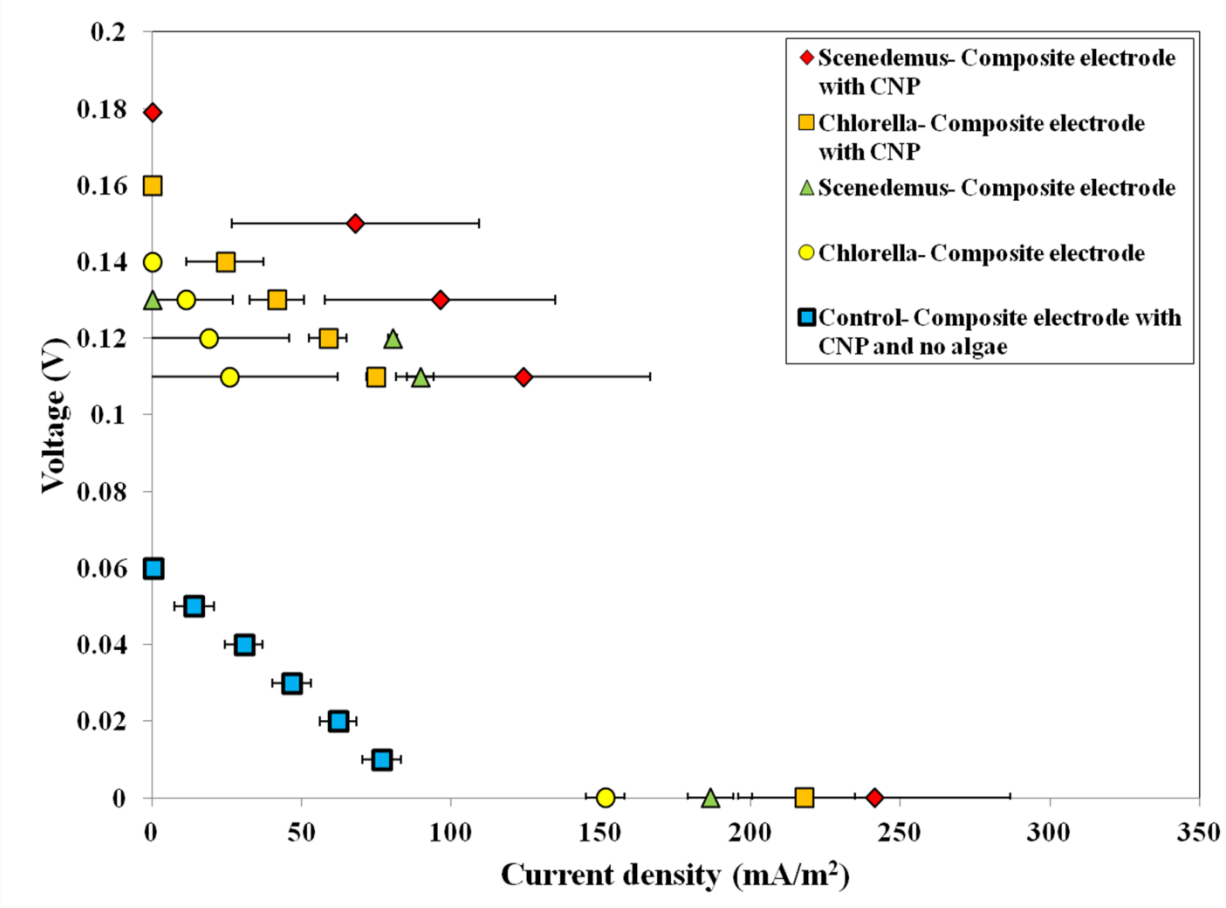

Figure 4.15 Polarization curves of composite electrode with attached CNP compared with composite electrodes without CNP for biocathode. Error bars represent standard deviation of current measurement.

4.6 Bio-batteries with coupled bionaode and biocathode

A complete bio-battery setup combined the bioanode containing bacteria and the biocathode containing algae. Composite electrode with immobilized bacteria was introduced in the bioanode chamber while the composite electrode with CNP coating was introduced in the biocathode chamber containing *Chlorella vulgaris* suspended in the solution.

4.6.1 Cell potential of complete bio-battery

The complete bio-battery was setup and its potential increased due to the growth of microbes and its interaction with the electrodes. The cell potential was allowed to stabilize, after which polarization and EIS experiments were conducted. Figure 4.16 shows the open circuit potential of the complete bio-battery setup. The open circuit potentials of the complete bio-battery setups were reproducible with voltages ranging between 0.47 V and 0.37 V.

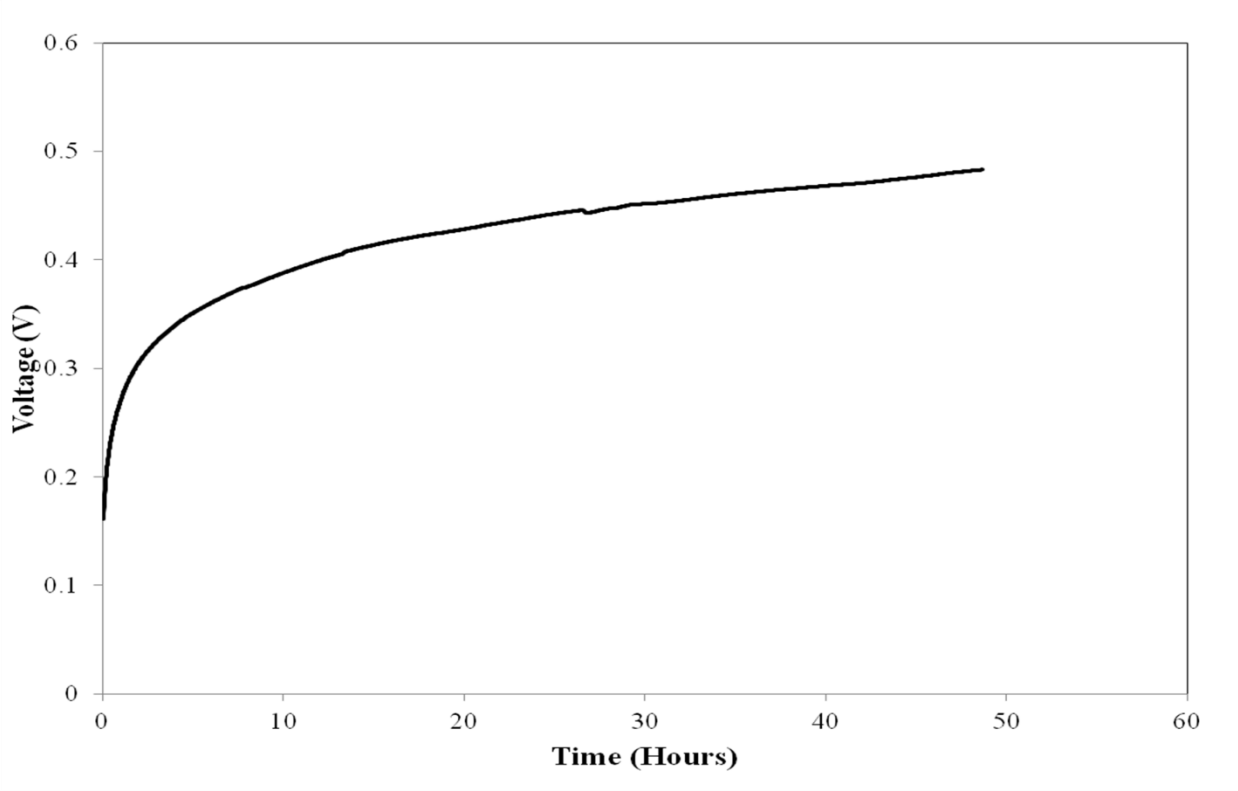

Figure 4.16 Open circuit potential of the complete bioanode-biocathode battery.

4.6.2 Polarization and power density curve

The polarization and current density curves of the complete bio-battery setup are shown in Figure 4.17. The average current and power densities achieved were 298 mA/m^2 and 43 mW/m^2 respectively. The current and power density measurements are represented with standard deviation error bars.

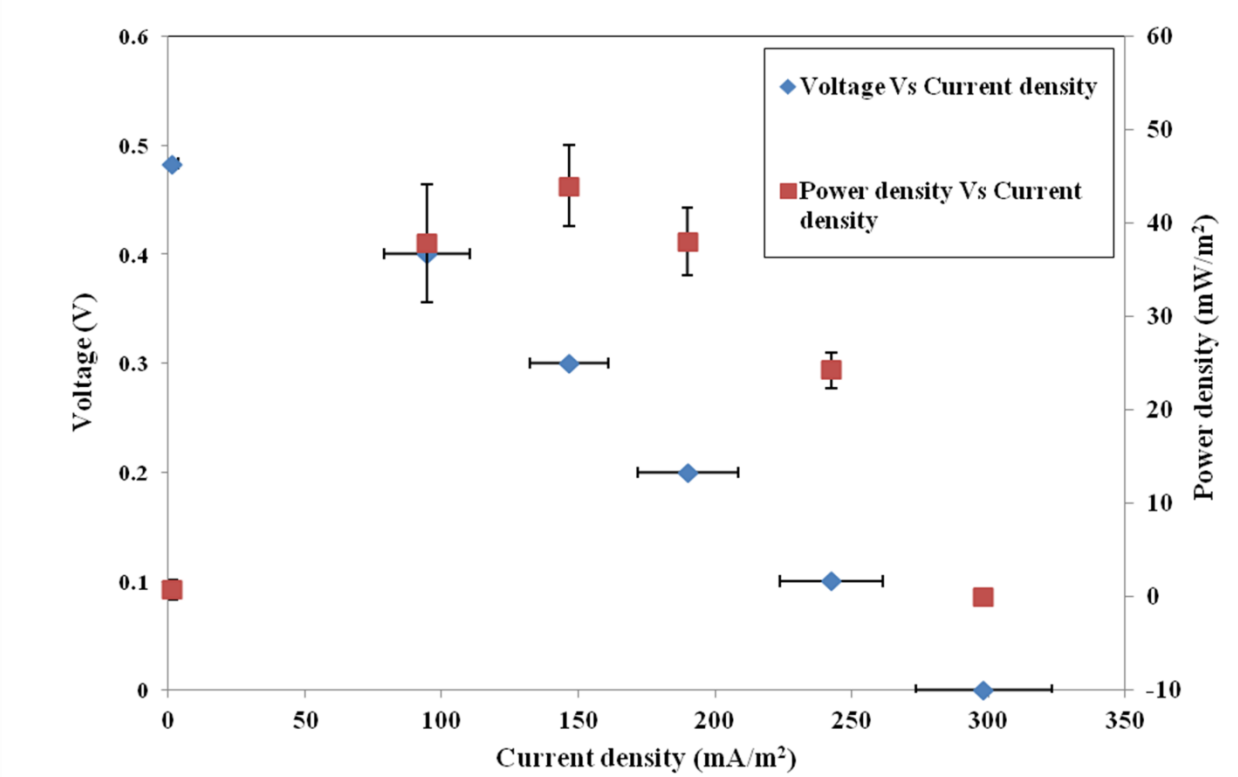

Figure 4.17 Polarization and power density curves of the complete bioanode-biocathode battery. Error bars represent standard deviation of current and power measurements.

4.6.3 EIS analysis with model fitting

Electrochemical Impedance Spectroscopy tests were conducted for the bioanode, biocathode and complete bio-battery setups. Reference electrodes were placed in the anode and cathode chambers. The membrane's contribution to ohmic resistance was determined by testing the bioanode with respect to the reference electrode placed in the biocathode chamber (three

electrode configuration) or vice versa and subtracting it with the ohmic resistance contributed by the bioanode or biocathode alone. It was determined that the membrane contributed to approximately 91 percent of the overall ohmic resistance of the fuel cell. Figure 4.18 shows the nyquist plots of the bioanode, biocathode and the complete bio-battery setup. Potentiostatic EIS experiments at steady state cell potentials (OCV) with amplitude of 10 mV and frequency range of 100 kHz to 0.1 Hz were conducted. Model 1 from Figure 4.12 was used to fit the points and determine the resistances. The biocathode and the complete bio-battery setup contributed the highest resistance (Large nyquist plots), with the bioanode (inset of Figure 4.18) being almost negligible.

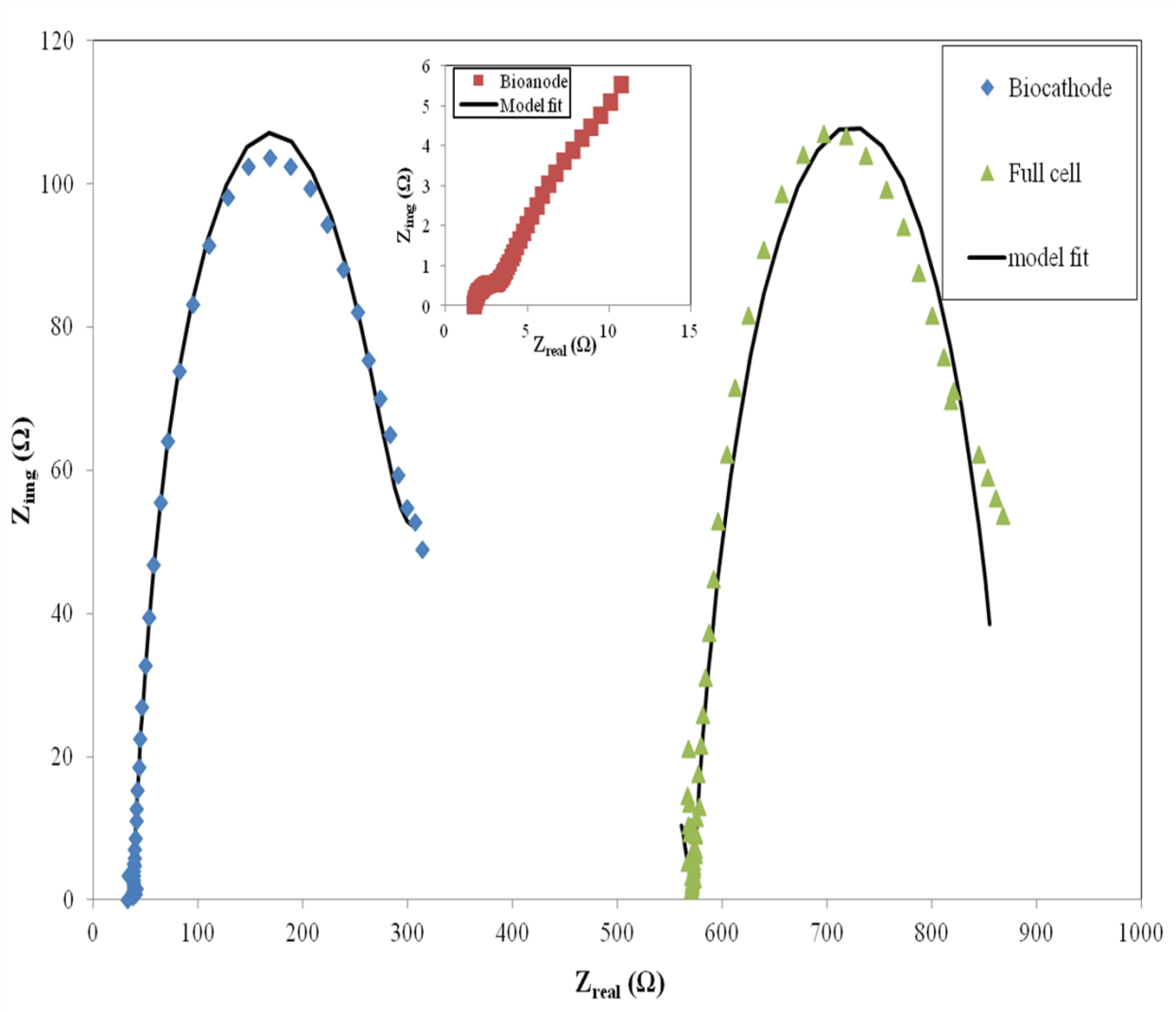

Figure 4.18 Nyquist plots of bioanode, biocathode and complete bio-battery setups with model fits. Potentiostatic EIS tests were done at steady state cell potentials (open circuit) with an amplitude of 10 mV and 100 to 0.1 Hz frequency. Bioanode and Biocathode impedance spectra were recorded using a three electrode configuration while the complete bio-battery setup's impedance spectra were recorded using a two electrode mode between the anode and the cathode.

4.6.4 Ohmic resistance contribution of individual chambers

The performance of dual chambered biological fuel cells are generally affected by high ohmic resistances in the system (Ramasamy *et al.*, 2008). Ohmic resistance is primarily present across the membrane or the liquid junction and also to a certain extent based on the ionic concentration in the anode and cathode (Godwin, 2011). The ohmic resistance contributions of the bioanode, biocathode and the complete bio-battery setups are shown in Figure 4.19. The ohmic resistance of the bioanode (~2 Ω) was lower than the biocathode (~60 Ω). This is due to the lower growth rate of algae compared to the bacteria or other electron donor species in the bioanode (Mitra and Hill, 2012). Moreover, the lower performance of the fuel cells when using algae biocathodes is primarily because of membrane biofouling and oxygen permeation through membrane (Chae *et al.*, 2007). In general, the photosynthetic biocathodes and the membrane are the major limiting factors in a complete bio-battery setup.

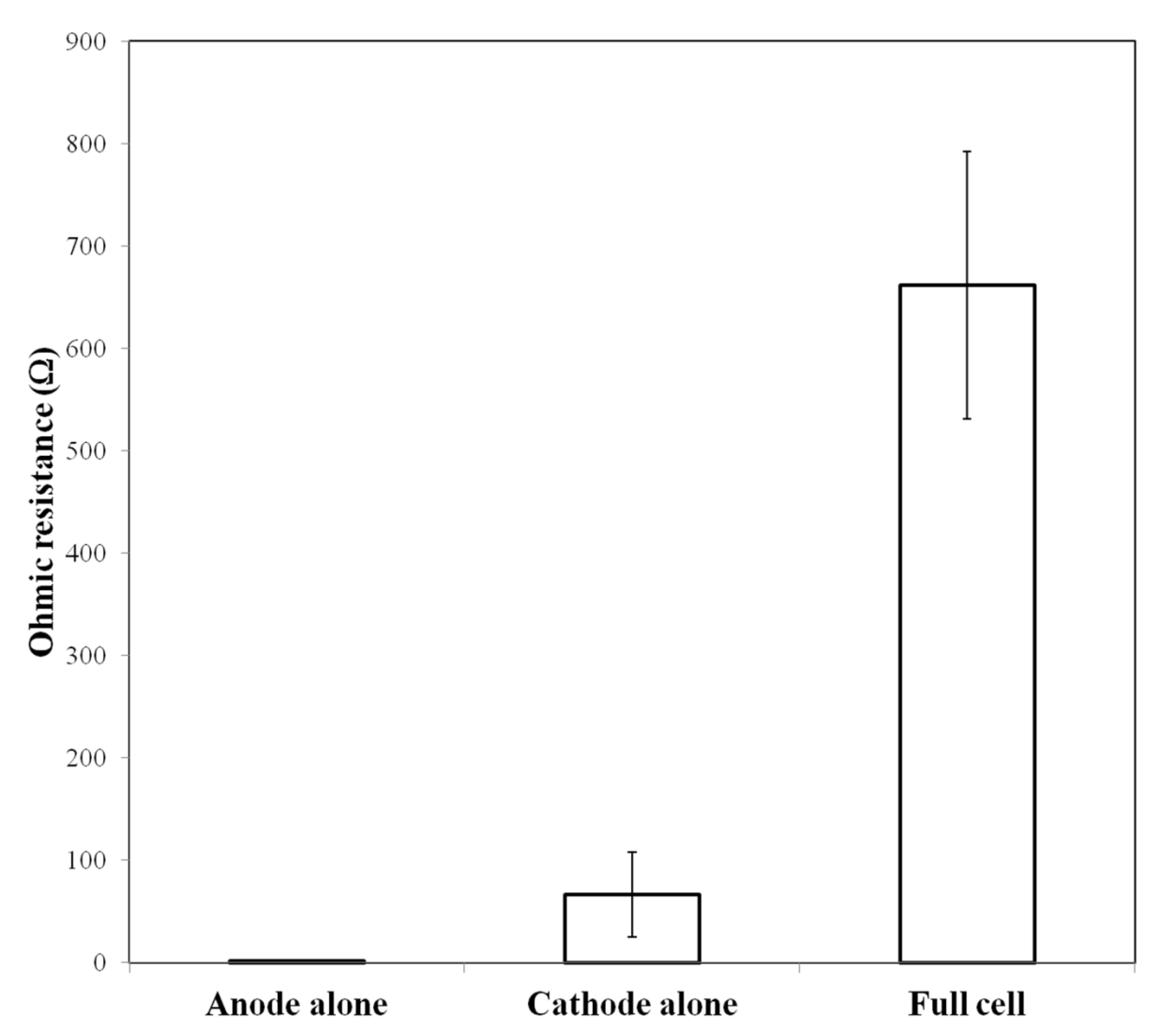

Figure 4.19 Ohmic resistance contribution of the bioanode, biocathode and complete bio-battery setups. Error bars represent standard deviation. Ohmic resistance contribution of the anode, cathode and entire bio-battery was calculated using reference electrodes placed in both the chambers.

5. SUMMARY, CONCLUSIONS AND RECOMMENDATIONS

5.1 Summary

The composite electrodes with immobilized bacteria (CNP-bacteria paste) setup produced higher current than other control configurations containing bacteria suspended in the solution. Moreover, it was determined, through EIS analysis, that the charge transfer resistance accounted for nearly 80% of the internal resistance in the bioanodes and this was reduced by approximately 53% by using composite electrodes with immobilized bacteria (CNP-bacteria paste). This is in line with the hypothesis that the immobilization of mediator and bacteria directly on the surface of the electrode would facilitate the transfer of charge from the bacterial cells to the electrode by reducing the charge transfer resistance.

The use of composite electrodes with CNP coating helped to improve the power generation in photosynthetic biocathodes compared with plain composite electrodes. This result is in line with the hypothesis that carbon nanoparticles increase the surface area for microbial adhesion and improve the conductivity of composite electrodes. EIS analysis on complete bio-battery setup showed that the biocathode and the membrane were the major limiting factors due to bio-fouling and permeation of oxygen into the bioanode chamber through the membrane.

5.2 Conclusions

The composite electrodes were prepared by polymerizing pyrrole and methylene blue on the surface of stainless steel mesh. The bacteria (*Escherichia coli K-12*) were subsequently immobilized on the composite electrode. The composite electrodes with immobilized bacteria (CNP-bacteria paste) achieved maximum current and power densities of 1645 mA/m^2 and 378 mW/m^2, respectively, when incorporated into the bioanode. The current and power densities of

this electrode were almost 53% and 69% more than other configurations, which could be attributed to the reduced charge transfer resistance in the bioanode. Specifically, it was concluded that the immobilization of bacteria onto the anode decreased the resistance to the transfer of charge from the bacteria to anode by approximately 53%, when compared to bacteria suspended in solution. These findings were confirmed through an Electrochemical Impedance Spectroscopy analysis with model fitting. This analysis also showed that the charge transfer, from bacteria to anode, is the most significant component of the bioanode's internal resistance. It was also determined that the carbon nanoparticles aided electron transfer by slightly improving the power output of the bioanode. The technique of bacteria immobilization did not inhibit bacterial growth which was supported by the glucose analysis experiment for biochemical activity.

The composite electrodes with carbon nanoparticles coating were tested in biocathodes containing photosynthetic microalgae. This electrode configuration achieved approximately 23% more current density than composite electrodes without CNP coating. This increase could be attributed to the increased surface area and improved conductivity by the carbon nanoparticles. Two species of photosynthetic microalgae were also tested, *Chlorella vulgaris* and *Scenedesmus sp.* It was determined that *Chlorella vulgaris* had a higher growth rate (determined by spectrophotometric analysis) and produced reproducible results. This indicates that the enhanced growth rate caused a uniform formation of bio-film on the electrode surface that attributed to the performance increase.

The bioanode and biocathodes were coupled to form a complete bio-battery. The bioanode was based on *Escherichia coli* metabolizing glucose and the biocathode contained *Chlorella vulgaris* for photosynthesis. The complete bio-battery setup achieved maximum current and

power densities of 316 mA/m^2 and 47 mW/m^2 respectively. EIS analysis found that the resistance was higher in the biocathode than in the bioanode and the membrane contributed to approximately 91% of the overall ohmic resistance.

5.3 Recommendations

There is a large knowledge gap regarding photosynthetic biocathodes. Their mechanism of electron transfer and current generation is not been clearly understood. More in-depth analysis of photosynthetic biocathodes has to be done to understand the electron transfer mechanism. Cyanobacteria, a different species of photosynthetic microrganism should be examined for cathodic current generation. Other species of bacteria that generate anodic current with or without mediators should be studied and tested. *Shewanella oneidensis* and *Geobacter sulfurreducens* do not require mediators for the transfer of electrons from their cells to the electrode and are worthy of investigation. In this research, the fuel cells were operated in batch mode. Future research should focus on continuous mode of operation of the fuel cells for long term viability and better performance.

High surface area electrodes can be designed and tested to improve the performance and economics of the MFCs. Nanoparticles such as Carbon Nano Tubes (CNT) could be embedded on the electrode surface to increase the surface area for bacterial adhesion and examined. The thickness of these coatings should also be measured. Titanium is an alternative to stainless steel and can be tested as electrode materials in MFCs. Most researchers use the geometric or projected surface of the electrodes to determine the current and power densities, which is not the true surface area. The true surface areas of the porous electrodes can be determined through BET and other analysis. Moreover, a Membrane Electrode Assembly (MEA) can be designed to

reduce the resistance caused due to the separation distance between the electrodes and the membrane. Lower resistance membranes can also be used to further increase power generation.

In this research, methylene blue was used as the redox mediator. Other redox compounds such as methyl orange, methyl red and neutral red can be investigated for performance enhancement of the bio-batteries. Teflon^{tm}, which was used as a binder, was found to inhibit the performance of the bio-battery since it is an electrical insulator. Alternatives to Teflon^{tm} such as Nafion^{tm} could be tested. Other methods of bacteria immobilization such as using sodium alginate and latex should be tested.

6. REFERENCES

Aelterman, P., Versichele, M., Marzorati, M., Boon, N., & Verstraete, W. (2008). Loading rate and external resistance control the electricity generation of microbial fuel cells with different three-dimensional anodes. *Bioresource Technology, 99*(18), 8895-8902.

Chae, K. J., Choi, M., Ajayi, F. F., Park, W., Chang, I. S., & Kim, I. S. (2007). Mass Transport through a Proton Exchange Membrane (Nafion) in Microbial Fuel Cells†. *Energy & Fuels, 22*(1), 169-176.

Chen, S., Chen, Y., He, G., He, S., Schröder, U., & Hou, H. (2012). Stainless steel mesh supported nitrogen-doped carbon nanofibers for binder-free cathode in microbial fuel cells. *Biosensors and Bioelectronics, 34*(1), 282-285.

Cheng, S., Liu, H., & Logan, B. E. (2006). Increased performance of single-chamber microbial fuel cells using an improved cathode structure. *Electrochemistry Communications, 8*(3), 489-494.

Dumas, C., Basseguy, R., & Bergel, A. (2008). Electrochemical activity of< i> Geobacter sulfurreducens</i> bio-films on stainless steel anodes. *Electrochimica Acta, 53*(16), 5235-5241.

Dumas, C., Mollica, A., Féron, D., Basséguy, R., Etcheverry, L., & Bergel, A. (2007). Marine microbial fuel cell: use of stainless steel electrodes as anode and cathode materials. *Electrochimica acta, 53*(2), 468-473.

Fan, Y., Sharbrough, E., & Liu, H. (2008). Quantification of the internal resistance distribution of microbial fuel cells. *Environmental science & technology, 42*(21), 8101-8107.

Fan, Y., Xu, S., Schaller, R., Jiao, J., Chaplen, F., & Liu, H. (2011). Nanoparticle decorated anodes for enhanced current generation in microbial electrochemical cells. *Biosensors and Bioelectronics, 26*(5), 1908-1912.

Freguia, S., Rabaey, K., Yuan, Z., & Keller, J. (2008). Sequential anode–cathode configuration improves cathodic oxygen reduction and effluent quality of microbial fuel cells. *Water research, 42*(6), 1387-1396.

Ghasemi, M., Wan Daud, W. R., Ismail, M., Rahimnejad, M., Ismail, A. F., Leong, J. X., . . . Ben Liew, K. (2012). Effect of pre-treatment and biofouling of proton exchange membrane on microbial fuel cell performance. *International Journal of Hydrogen Energy*.

Godwin, J. (2011). *Immobilized mediator electrodes for microbial fuel cells.* University of Saskatchewan.

Godwin, J. M., & Evitts, R. (2011). Polypyrrole/poly (methylene blue) composite electrode films on stainless steel. *ECS Transactions, 33*(27), 181-188.

González del Campo, A., Cañizares, P., Rodrigo, M. A., Fernández, F. J., & Lobato, J. (2013). Microbial fuel cell with an algae-assisted cathode: A preliminary assessment. *Journal of Power Sources*.

He, Z., & Mansfeld, F. (2009). Exploring the use of electrochemical impedance spectroscopy (EIS) in microbial fuel cell studies. *Energy & Environmental Science, 2*(2), 215-219.

He, Z., Minteer, S. D., & Angenent, L. T. (2005). Electricity generation from artificial wastewater using an upflow microbial fuel cell. *Environmental science & technology, 39*(14), 5262-5267.

Hoffman, A., Suresh, S., Evitts, R., Kennell, G., & Godwin, J. (2013). Dual-chambered bio-batteries using immobilized mediator electrodes. *Journal of Applied Electrochemistry*, 1-8.

Hosseini, M. G., & Ahadzadeh, I. (2012). A dual-chambered microbial fuel cell with Ti/nano-TiO2/Pd nano-structure cathode. *Journal of Power Sources*.

Karyakin, A. A., Karyakina, E. E., & Schmidt, H. L. (1999). Electropolymerized azines: a new group of electroactive polymers. *Electroanalysis, 11*(3), 149-155.

Kim, J. H., Park, W., & Kim, S. (2011). Immobilized Polyviologen as an Effective Redox Mediator for Microbial Fuel Cells. *Bulletin of the Korean Chemical Society, 32*(11), 3849-3850.

Lies, D. P., Hernandez, M. E., Kappler, A., Mielke, R. E., Gralnick, J. A., & Newman, D. K. (2005). Shewanella oneidensis MR-1 uses overlapping pathways for iron reduction at a distance and by direct contact under conditions relevant for biofilms. *Applied and Environmental Microbiology, 71*(8), 4414-4426.

Logan, B., Cheng, S., Watson, V., & Estadt, G. (2007). Graphite fiber brush anodes for increased power production in air-cathode microbial fuel cells. *Environmental science & technology, 41*(9), 3341-3346.

Logan, B. E. (2009). Exoelectrogenic bacteria that power microbial fuel cells. *Nature Reviews Microbiology, 7*(5), 375-381.

Logan, B. E., Hamelers, B., Rozendal, R., Schröder, U., Keller, J., Freguia, S., . . . Rabaey, K. (2006). Microbial fuel cells: methodology and technology. *Environmental science & technology, 40*(17), 5181-5192.

Luckarift, H. R., Sizemore, S. R., Roy, J., Lau, C., Gupta, G., Atanassov, P., & Johnson, G. R. (2010). Standardized microbial fuel cell anodes of silica-immobilized Shewanella oneidensis. *Chemical Communications, 46*(33), 6048-6050.

Manohar, A. K., Bretschger, O., Nealson, K. H., & Mansfeld, F. (2008). The use of electrochemical impedance spectroscopy (EIS) in the evaluation of the electrochemical properties of a microbial fuel cell. *Bioelectrochemistry, 72*(2), 149-154.

Manohar, A. K., & Mansfeld, F. (2009). The internal resistance of a microbial fuel cell and its dependence on cell design and operating conditions. *Electrochimica Acta, 54*(6), 1664-1670.

Mao, Y., Zhang, L., Li, D., Shi, H., Liu, Y., & Cai, L. (2010). Power generation from a biocathode microbial fuel cell biocatalyzed by ferro/manganese-oxidizing bacteria. *Electrochimica Acta, 55*(27), 7804-7808.

Martins, J., Reis, T., Bazzaoui, M., Bazzaoui, E., & Martins, L. (2004). Polypyrrole coatings as a treatment for zinc-coated steel surfaces against corrosion. *Corrosion Science, 46*(10), 2361-2381.

Min, B., Cheng, S., & Logan, B. E. (2005). Electricity generation using membrane and salt bridge microbial fuel cells. *Water research, 39*(9), 1675-1686.

Mitra, P., & Hill, G. A. (2012). Continuous microbial fuel cell using a photoautotrophic cathode and a fermentative anode. *The Canadian Journal of Chemical Engineering, 90*(4), 1006-1010.

Oh, S.-E., & Logan, B. E. (2006). Proton exchange membrane and electrode surface areas as factors that affect power generation in microbial fuel cells. *Applied microbiology and biotechnology, 70*(2), 162-169.

Park, D. H., & Zeikus, J. G. (2003). Improved fuel cell and electrode designs for producing electricity from microbial degradation. *Biotechnology and bioengineering, 81*(3), 348-355.

Powell, E., Evitts, R., Hill, G., & Bolster, J. (2011). A microbial fuel cell with a photosynthetic microalgae cathodic half cell coupled to a yeast anodic half cell. *Energy Sources, Part A: Recovery, Utilization, and Environmental Effects, 33*(5), 440-448.

Prieto-Simón, B., & Fàbregas, E. (2004). Comparative study of electron mediators used in the electrochemical oxidation of NADH. *Biosensors and Bioelectronics, 19*(10), 1131-1138.

Qiao, Y., Li, C. M., Bao, S.-J., & Bao, Q.-L. (2007). Carbon nanotube/polyaniline composite as anode material for microbial fuel cells. *Journal of Power Sources, 170*(1), 79-84.

Rabaey, K., & Verstraete, W. (2005). Microbial fuel cells: novel biotechnology for energy generation. *Trends in Biotechnology, 23*(6), 291-298. doi: http://dx.doi.org/10.1016/j.tibtech.2005.04.008

Ramasamy, R. P., Ren, Z., Mench, M. M., & Regan, J. M. (2008). Impact of initial biofilm growth on the anode impedance of microbial fuel cells. *Biotechnology and bioengineering, 101*(1), 101-108.

Ringeisen, B. R., Henderson, E., Wu, P. K., Pietron, J., Ray, R., Little, B., . . . Jones-Meehan, J. M. (2006). High power density from a miniature microbial fuel cell using Shewanella oneidensis DSP10. *Environmental science & technology, 40*(8), 2629-2634.

Schröder, U., Nießen, J., & Scholz, F. (2003). A generation of microbial fuel cells with current outputs boosted by more than one order of magnitude. *Angewandte Chemie International Edition, 42*(25), 2880-2883.

Silber, A., Hampp, N., & Schuhmann, W. (1996). Poly (methylene blue)-modified thick-film gold electrodes for the electrocatalytic oxidation of NADH and their application in glucose biosensors. *Biosensors and Bioelectronics, 11*(3), 215-223.

Vernitskaya, T., & Efimov, O. (1997). Polypyrrole: a conducting polymer (synthesis, properties, and applications). *Uspekhi khimii, 66*(5), 489-505.

Wagner, R. C., Porter-Gill, S., & Logan, B. E. (2012). Immobilization of anode-attached microbes in a microbial fuel cell. *AMB Express, 2*(1), 1-6.

Walter, X. A., Greenman, J., & Ieropoulos, I. A. (2013). Oxygenic phototrophic biofilms for improved cathode performance in microbial fuel cells. *Algal Research*.

Wang, X., Cheng, S., Feng, Y., Merrill, M. D., Saito, T., & Logan, B. E. (2009). Use of carbon mesh anodes and the effect of different pretreatment methods on power production in microbial fuel cells. *Environmental science & technology*, *43*(17), 6870-6874.

Wei, J., Liang, P., & Huang, X. (2011). Recent progress in electrodes for microbial fuel cells. *Bioresource Technology, 102*(20), 9335-9344. doi: http://dx.doi.org/10.1016/j.biortech.2011.07.019

Wen, Z., Ci, S., Mao, S., Cui, S., Lu, G., Yu, K., . . . Chen, J. (2013). TiO2 nanoparticles-decorated carbon nanotubes for significantly improved bioelectricity generation in microbial fuel cells. *Journal of Power Sources*.

XI, M.-y., & SUN, Y.-p. (2008). Preliminary study on E. coli microbial fuel cell and on-electrode taming of the biocatalyst. *过程工程学报, 8*(6).

Yan, Z., Wang, M., Huang, B., Liu, R., & Zhao, J. (2013). Graphene Supported Pt-Co Alloy Nanoparticles as Cathode Catalyst for Microbial Fuel Cells. *Int. J. Electrochem. Sci, 8*, 149-158.

Yuan, Y., Ahmed, J., Zhou, L., Zhao, B., & Kim, S. (2011). Carbon nanoparticles-assisted mediator-less microbial fuel cells using< i> Proteus vulgaris</i>. *Biosensors and Bioelectronics, 27*(1), 106-112.

Yuan, Y., Jeon, Y., Ahmed, J., Park, W., & Kim, S. (2009). Use of carbon nanoparticles for bacteria immobilization in microbial fuel cells for high power output. *Journal of The Electrochemical Society, 156*(10), B1238-B1241.

Zhang, F., Saito, T., Cheng, S., Hickner, M. A., & Logan, B. E. (2010). Microbial fuel cell cathodes with poly (dimethylsiloxane) diffusion layers constructed around stainless steel mesh current collectors. *Environmental science & technology, 44*(4), 1490-1495.

Zhao, F., Slade, R. C., & Varcoe, J. R. (2009). Techniques for the study and development of microbial fuel cells: an electrochemical perspective. *Chemical Society Reviews, 38*(7), 1926-1939.